Master Thesis

Analysis of a two species TASEP as a model for heterogeneous transport on microtubules

Author:
Alessandro Giacomo Bottero

Supervisor:
Prof. Dr. Erwin Frey

Ludwig-Maximilians-Universität
München

Master Programme

Theoretical and Mathematical Physics

June 2, 2017

Abstract

We investigate a modified version of the one dimensional totally asymmetric simple exclusion process (TASEP). In particular, motivated by experimental findings of functional heterogeneity of motor proteins, we analyze a TASEP where heterogeneity for the hopping rate is allowed, as an effective way to model the dynamics of molecular motors with different velocities along microtubules. Specifically, we consider the case of a lattice with open boundaries and with two species of particles – a fast and a slow one – and we focus on the densities and current profiles in the steady state. In order to obtain these quantities from the master equation, we first perform a mean field analysis, which has been proven successful for the classic TASEP. To the contrary, here we find that the mean field results disagree consistently with our Monte Carlo simulations. Hence, we develop a refined mean field theory, which turns out to be very successful and in good agreement with the simulations. With this result at hand, we then extend our model to introduce Langmuir kinetics to the system, in order to better model the real biological process of motor dynamics. The simulations of this new stochastic system reveal an extremely interesting phenomenology – which includes the emergence of domain walls, phase coexistence and species segregation – and a rich phase space, whose analysis and further exploration may be the object of future studies.

Contents

Introduction

Microtubules are cylindrical structures which assemble by polymerization of dimers of alpha and beta tubulin [1]. They are found in the cell's cytoplasm, and are fundamental components of eukaryotic cells' cytoskeleton [2, 3]. Among their other functions, microtubules provide a way for organelles to be moved around the cell [4]. This active biological transport is achieved by means of molecular motors: enzymes like kinesin which, thanks to the conversion of chemical energy into mechanical work, can move unidirectionally along the microtubule [5].

Such a *walking* process happens in a random Poisson-like fashion, is mostly constrained to a single lane of the microtubule, and obeys exclusion: two motors cannot be simultaneously attached to the same tubuline site [6]. Thanks to these properties of the molecular motors dynamics along microtubules, an ideal candidate for a minimal model to study such process theoretically is the *Totally Asymmetric Simple Exclusion Process* (TASEP). This model is a paradigmatic example in non equilibrium statistical physics, and it has been widely studied in literature, as reviewd, for example, by Chou, Mallick and Zia in [5].

However, the standard TASEP allows only one kind of motor (i.e. all the particles in this model have the same avarage velocity), whereas, in biological systems, it is possible that different motors walk along the same microtubule. Moreover, in a recent study by Reddy et al. [7], it has been found that even the same kind of motors can exhibit functional heterogeneity, meaning that, even though they are chemically identical, they can show different behaviours and move with different average velocities.

These findings suggest that an interesting and biologically relevant model to study would be a heterogeneous TASEP, where the particles are allowed to have different velocities. In the first part of the thesis, therefore, we study in detail such a model, in the particular case of two species of particles, trying to obtain the phase diagram at stationarity. Once we have a better understanding of the two species TASEP, in the final part of the thesis, we move on studying what happens when such process is coupled with Langmuir kinetics.

Chapter 1

Heterogeous TASEP

1.1 The standard TASEP

Before beginning to analyze the model that we are interested in – i.e. the heterogeneous TASEP – it is useful to briefly recall the basic results for the standard TASEP. In particular, we will focus on a 1D open boundaries problem (see Figure 1.1).

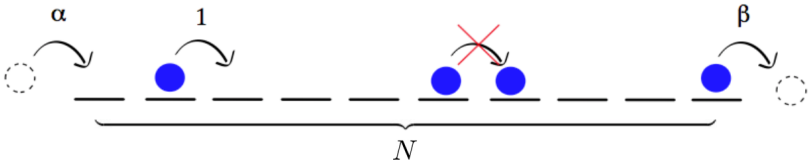

Figure 1.1: Sketch of a standard 1D TASEP on an open lattice of lenght N.

The TASEP is a stochastic process and, more precisely, a Markov process, where particles enter the lattice from the first site with rate α, then hop forward on the lattice with hopping rate $h = 1$, one site at the time, and only if the next lattice site is empty: because of the exclusion property, each site can be occupied at most by one particle at the time. Finally, once a particle has reached the last lattice site, it exits the lattice with rate β. Under these assumptions it is straightforward to derive the evolution equation for the average occupation of each site. In the bulk one has:

$$\frac{d}{dt}\langle n_i \rangle = \langle n_{i-1}(1-n_i)\rangle - \langle n_i(1-n_{i+1})\rangle = \langle j_{i-1}\rangle - \langle j_i\rangle \qquad (1.1)$$

where n_i is the occupation of the i-th site, and $\langle j_i\rangle := \langle n_i(1-n_{i+1})\rangle$ is the

average current from site i to site $i+1$. For what concerns the first and the last lattice site, on the other hand, one finds, respectively:

$$\begin{aligned} \frac{d}{dt}\langle n_1\rangle &= \alpha\langle 1-n_1\rangle - \langle n_1(1-n_2)\rangle \\ \frac{d}{dt}\langle n_N\rangle &= \langle n_{N-1}(1-n_N)\rangle - \beta\langle n_N\rangle \end{aligned} \tag{1.2}$$

From these equations we see that, in order to compute the time evolution of the average occupation, we need also the higher moments of its distribution. One way to go around this inconvenience and be able to compute the steady state density and average current would be to perform a mean field approximation and disregard possible contributions of the correlations. However, even though such an approach leads to a good approximation and a

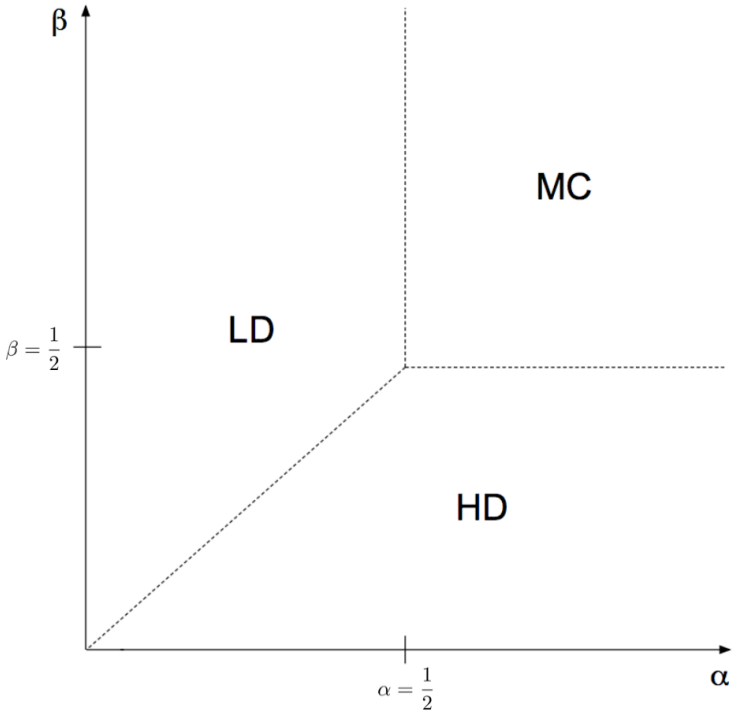

Figure 1.2: Steady state Phase diagram in the limit $N \to \infty$ of a standard TASEP.

correct phase diagram in the hydrodynamic limit – as Chou, Mallick and Zia explain in their review [5] – in this particular case an exact solution can be

obtained by means of a matrix ansatz [8, 9, 5]. In the limit of $N \to \infty$, this solution for the steady state distributions yields the phase diagram drawn in Figure 1.2: three phases are possible and the transitions between them is driven by the entrance end exit rates. For low α and high β the system is in a low density (LD) phase, for low β and high α it is in a high density phase (HD), while for both α and β bigger than 1/2, the system is in the so called maximal current (MC) phase, in which, as the name sugests, the average bulk current assumes its maximum value. The transitions between the MC phase and the LD and between the MC and HD are continuous, while the one between HD and LD phases is not. More quantitatively, the value of the density in the three phases is given by:

$$\begin{aligned} \rho_{LD}(\alpha) &= \alpha \\ \rho_{MC} &= \frac{1}{2} \\ \rho_{HD}(\beta) &= 1 - \beta \end{aligned} \tag{1.3}$$

where we called ρ the average density: $\rho := \langle n \rangle$. More details about the phase diagram of the standard TASEP can be found, for example, in [5, 10, 11].

1.2 Two species TASEP

After revisiting the basic properties of the standard TASEP, we are now ready to introduce the model that we are interested in.

As anticipated in the introduction, the basic model that we will focus on in the first part of the thesis is a standard one dimensional TASEP with open boundaries, where we allow heterogeneity in the hopping rate. The defining properties of such model are summarized in Figure 1.3: two species of particles can enter the 1D lattice – of lenght N – on the left with total entry rate α, then they can only hop forward with hopping rates $h_1 = 1$ for the first species and $h_2 = q < 1$ for the second one. Both species respect the exclusion principle: a particle can hop to the next site only if this one is not occupied by any particle. Finally, once a particle reaches the last lattice site on the right, it leaves the system at rate β. The last free parameter of the model is the relative fraction of *fast* particles (particles with the bigger hopping rate): $p \in (0, 1)$, which enters in the single entrance rates for the two different species: the fast particles enter the system at rate $p \cdot \alpha$, while the

slow ones at rate $(1-p)\cdot\alpha$. Note that the values $p=1$ or $p=0$ have been excluded, because, for $p=1$ or $p=0$, we recover, respectively, a standard TASEP or a standard TASEP with reduced hopping rate $q<1$.

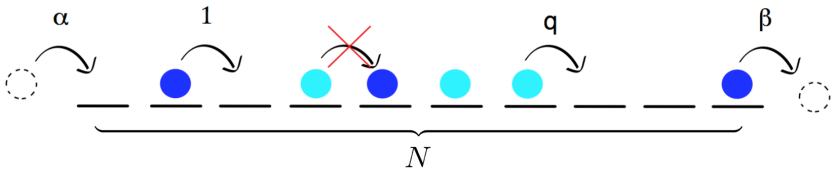

Figure 1.3: Sketch of the 2 species TASEP model.

A configuration $\mathcal{C}$ of the system is defined by the occupation state of each lattice site (unoccupied, occupied by a fast particle, or occupied by a slow particle). As for the standard TASEP, this is also a Markov process, and the time evolution of the probability of a particular configuration $\tilde{\mathcal{C}}$ is given by the master equation:

$$\frac{d}{dt}P(\tilde{\mathcal{C}}) = \sum_{\{\mathcal{C}\}}\Big[\omega(\mathcal{C}\to\tilde{\mathcal{C}})P(\mathcal{C}) - \omega(\tilde{\mathcal{C}}\to\mathcal{C})P(\tilde{\mathcal{C}})\Big] \tag{1.4}$$

where the sum runs over all the 3^N possible configurations of the system, and $\omega(\mathcal{C}\to\tilde{\mathcal{C}})$ and $\omega(\tilde{\mathcal{C}}\to\mathcal{C})$ are, respectively, the probability – per unit of time – to go from the configuration $\mathcal{C}$ to $\tilde{\mathcal{C}}$ and the one to go from $\tilde{\mathcal{C}}$ to $\mathcal{C}$, both equal to 0 in case the two configurations differ in the occupation of more than one lattice site.

1.3 Mean Field Approximation

Our first goal is to derive an expression for the densities of the two species of particles and the respective currents in the stationary state.

For what concern the notation, we will call n_i the occupation state of the i-th site with respect to the fast particles: $n_i=1$ if the site is occupied by a fast particle and 0 otherwise, while m_i denotes the occupation with respect to the slow particles. Finally, in the following will be convenient to consider also the total occupation, which we will call τ_i (obviously, $\tau_i = n_i+m_i$). Once averaged, these occupations will be called, respectively, $\rho_i := \langle n_i\rangle$, $\mu_i := \langle m_i\rangle$ and $\theta_i := \langle\tau_i\rangle$.

This being said, we can now write down the evolution of the occupation variables. In the bulk we will have:

$$\begin{aligned}\frac{d}{dt}\rho_i &= \langle n_{i-1}(1-n_i-m_i)\rangle - \langle n_i(1-n_{i+1}-m_{i+1})\rangle \\ \frac{d}{dt}\mu_i &= q[\langle m_{i-1}(1-n_i-m_i)\rangle - \langle m_i(1-n_{i+1}-m_{i+1})\rangle]\end{aligned} \tag{1.5}$$

whereas the occupations on the first lattice site obey the following:

$$\begin{aligned}\frac{d}{dt}\rho_1 &= p\alpha\,\langle 1-n_1-m_1\rangle - \langle n_1(1-n_2-m_2)\rangle \\ \frac{d}{dt}\mu_1 &= (1-p)\alpha\,\langle 1-n_1-m_1\rangle - q\,\langle m_1(1-n_2-m_2)\rangle\end{aligned} \tag{1.6}$$

and, finally, for the last site, one finds:

$$\begin{aligned}\frac{d}{dt}\rho_N &= \langle n_{N-1}(1-n_N-m_N)\rangle - \beta\,\langle n_N\rangle \\ \frac{d}{dt}\mu_N &= q\,\langle m_{N-1}(1-n_N-m_N)\rangle - \beta\,\langle m_N\rangle\end{aligned} \tag{1.7}$$

From Eqs. (1.5)–(1.7), we see that, as expected, to compute the evolution of the densities, we need also the higher moments of the occupation variables. In order to circumvent this problem, our first attempt will be to perform a mean field analysis which has been shown to give quite accurate results in other cases, like the standard TASEP [9, 12], or the tandard TASEP coupled with Langmuir Kinetics [13]. Such analysis consists in neglecting the correlations between different sites of the lattice, so that we can write: $\langle \tau_i \tau_j\rangle \approx \langle \tau_i\rangle\,\langle \tau_j\rangle$.

1.3.1 Degrees of freedom

Before rewriting the equations (1.5)–(1.7) using the mean field assumption, it is interesting and useful to note that, under this hypothesis, the number of degrees of freedom at stationarity reduces from two to one, so that we only need to compute one of the three densities ρ_i, μ_i and θ_i in order to have all of them.

Because of particle conservation in the bulk, this result is true, and easily proven also without the need of the mean field assumption, for the total avarage number of particles in the system. Since there is no attachment or detachment of particles in the bulk, in fact, in the steady the quantity $\langle N_\rho/N_\mu\rangle$ (where N_ρ is the total number of particle of the first pecies in the lattice and N_μ the one of slow particles) will be given by $p(1-p)^{-1}$, since p is the relative probability of a fast particle to enter the lattice.

However, under the mean field hypothesis, this results holds also locally for each site, and not only for the total number of particles in the system. Intuitively, this is clear: in the stationary state, given that a site is occupied, we'll have a probability p that this particle is a fast one and a probability $(1-p)$ that is a slow one instead, so that, $\forall i$, $\rho_i = p\theta_i$ and $\mu_i = (1-p)\theta_i$.

This can also be proven more rigorously, for example in the following way. The density of, let's say, the fast particles at site i-th is given by:

$$\rho_i = \sum_{\{\mathcal{C}_i^1\}} P(\mathcal{C}_i^1) \tag{1.8}$$

where the sum runs over all the configurations $\mathcal{C}_i^1$ of the lattice where the site i-th is occupied by a fast particle (which we implicitely assumed to be the first species, hence the index 1), and $P(\mathcal{C}_i^1)$ is the probability of the particular configuration. Now we can focus on one of these configurations and, after some straightforward manipulations of the probabilities, write:

$$\begin{aligned} P(\mathcal{C}_i^1) &= P((\tau_j = k_j \forall j \neq i) \wedge \tau_i = 1) \\ &= P((\tau_j = k_j \forall j \neq i) \ \wedge \ \tau_i = 1 | (\tau_j = k_j \forall j \neq i) \wedge \tau_i \neq 0) P((\tau_j = k_j \forall j \neq i) \wedge \tau_i \neq 0) \end{aligned} \tag{1.9}$$

where τ_j is the occupation of the j-th site: $\tau_j = 0$ means that the site is empty, $\tau_j = 1$ means that it is occupied by a fast particle (first species) and $\tau_j = 2$ means that it is occupied by a slow one (second species), while the vector $(k_1, \ldots, k_{i-1}, k_{i+1}, \ldots, k_N) \in \{0,1,2\}^{N-1}$ is a fixed $(N-1)$ dimensional array.

If we now treat the occupations of different sites as independent events, the conditional probability in the second line of eq. (1.9) simplifies to:

$$P((\tau_j = k_j \forall j \neq i) \ \wedge \ \tau_i = 1 | (\tau_j = k_j \forall j \neq i) \wedge \tau_i \neq 0) \longrightarrow P(\tau_i = 1 | \tau_i \neq 0)$$

which is just the probability that, given a particle on the i-th site of the lattice, this is a fast one. And, in the stationary state, this is nothing else that the fraction of fast particles in the system, which is given by p.

So that we have proven that

$$P((\tau_j = k_j \ \forall \ j \neq i) \wedge \tau_i = 1) = pP((\tau_j = k_j \ \forall \ j \neq i) \wedge \tau_i \neq 0)$$

In the exact same way, one can show that:

$$P((\tau_j = k_j \ \forall \ j \neq i) \wedge \tau_i = 2) = (1-p)P((\tau_j = k_j \ \forall \ j \neq i) \wedge \tau_i \neq 0)$$

Therefore, putting all together, we find that in the mean field approximation the following holds:

$$\begin{aligned}\rho_i &= \sum_{\mathbf{k}\in\{0,1,2\}^{N-1}} P(\tau_j = k_j \ \forall\ j \neq i \wedge \tau_i = 1) \\ &= p \sum_{\mathbf{k}\in\{0,1,2\}^{N-1}} P(\tau_j = k_j \ \forall\ j \neq i \wedge \tau_i \neq 0)\end{aligned} \tag{1.10}$$

and, similarly:

$$\begin{aligned}\mu_i &= \sum_{\mathbf{k}\in\{0,1,2\}^{N-1}} P(\tau_j = k_j \ \forall\ j \neq i \wedge \tau_i = 2) \\ &= (1-p) \sum_{\mathbf{k}\in\{0,1,2\}^{N-1}} P(\tau_j = k_j \ \forall\ j \neq i \wedge \tau_i \neq 0)\end{aligned} \tag{1.11}$$

so that we see that $\rho_i/\mu_i = p(1-p)^{-1}$, which, with straightforward algebra, translates into:

$$\rho_i = p\theta_i \quad \wedge \quad \mu_i = (1-p)\theta_i \tag{1.12}$$

This proves our intuition about the fact that, if we neglect correlations between different sites, our theory has only one degree of freedom, the other one being determined by equations (1.12). In the following analysis, therefore, we will use this fact and concentrate only on the total density θ_i.

1.3.2 Stationary State distribution

We are now ready to compute the steady state distribution and the current for the total density in the mean field limit.

If we sum up the equations (1.5), (1.6) and (1.7) after setting to 0 the left hand side (we are interested in the steady state), apply the mean field assumption, and use the relations (1.12) that we just proved, we find that the evolution of the total density, respectively of the first lattice site, in the bulk and of the last site, is governed by the following equations:

$$\begin{aligned}0 &= \alpha(1-\theta_1) - [p + q(1-p)]\theta_1(1-\theta_2) \\ 0 &= \theta_{i-1}(1-\theta_i) - \theta_i(1-\theta_{i+1}) \\ 0 &= [p + q(1-p)]\theta_{N-1}(1-\theta_N) - \beta\theta_N\end{aligned} \tag{1.13}$$

looking at these equations, we immediately note that they can be rewritten so that they take the exact same form as the mean field equations of the standard TASEP:

$$\begin{aligned} 0 &= \alpha^*(1-\theta_1) - \theta_1(1-\theta_2) \\ 0 &= \theta_{i-1}(1-\theta_i) - \theta_i(1-\theta_{i+1}) \\ 0 &= \theta_{N-1}(1-\theta_N) - \beta^*\theta_N \end{aligned} \tag{1.14}$$

with the new entrance and exit parameters α^* and β^* defined by:

$$\alpha^* := \alpha[p+q(1-p)]^{-1} \quad \text{and} \quad \beta^* := \beta[p+q(1-p)]^{-1} \tag{1.15}$$

In a completely similar fashion we can also compute the total current in the bulk:

$$\begin{aligned} \langle j_i \rangle &= \langle n_i(1-\tau_{i+1}) \rangle + q \langle m_i(1-\tau_{i+1}) \rangle \overset{MF}{=} \\ &\overset{MF}{=} [p+q(1-p)]\theta_i(1-\theta_{i+1}) \end{aligned} \tag{1.16}$$

and we see that also the current assume the same form it has in the mean field analysis of the standard TASEP, *modulo* the factor $[p+q(1-p)]$.

What we have found, therefore, is that, in the mean field approximation, our model reduces to a standard TASEP with rescaled hopping rate $q^* = [p+q(1-p)]$, which is exactly what one would intuitively expect: if there is no correlation between the positions of fast and slow particles, one has nothing else that two TASEPs taking place on the same lattice, one consisting of a fraction p of particles, with hopping rate $h_1 = 1$, and the other consisting of a fraction $(1-p)$ of particles, with hopping rate $h_2 = q$, resulting in an effective hopping rate, for the total system, of $h_{eff} = ph_1+(1-p)h_2 = p+(1-p)q = q^*$.

Now, the behaviour of the TASEP in the steady state is well known [9], and from that it is straightforward to obtain the same knowledge for a TASEP with a reduced hopping rate. From equations (1.13) and (1.14), we can, therefore, easily draw the phase diagram of our model, at the steady state, in the mean field limit. What we obtain is the diagram shown in Figure 1.4, where MC stands for *Maximal Current* phase, LD for *Low Density* phase

and HD for *High Density* phase, with the densities in these three regions given by:

$$\theta_{LD}(\alpha) = \frac{\alpha}{q^*} = \frac{\alpha}{p + q(1-p)}$$

$$\theta_{MC} = \frac{1}{2} \tag{1.17}$$

$$\theta_{HD}(\beta) = 1 - \frac{\beta}{q^*} = 1 - \frac{\beta}{p + q(1-p)}$$

and where, exactly as in the standard TASEP, the transitions between the

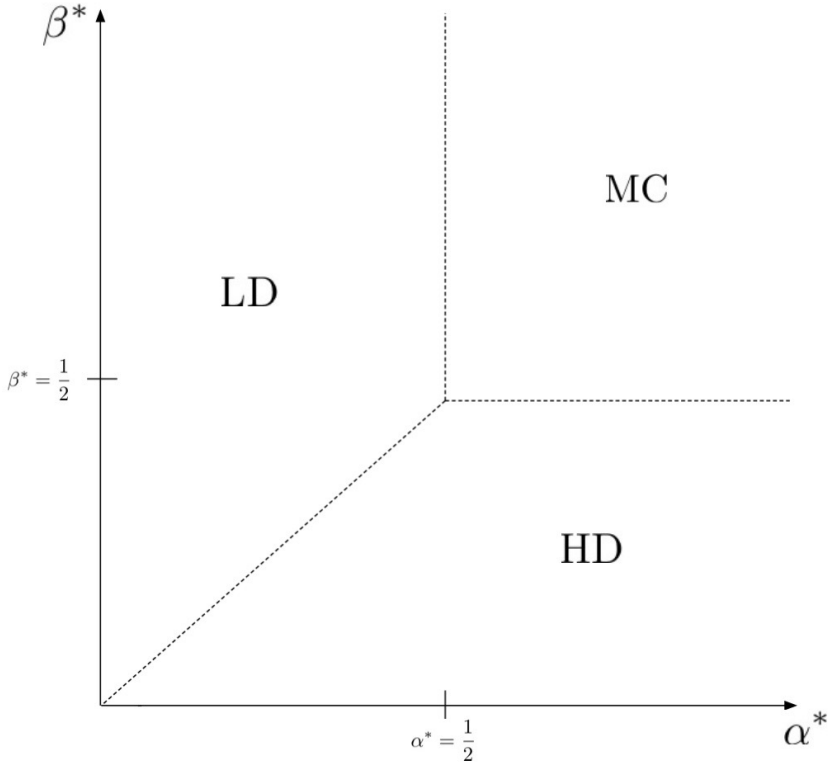

Figure 1.4: Mean Field Phase diagram for the 2-TASEP

HD phase and the MC phase and between the LD phase and MC phase are continuous, while the one between the LD and the HD phases is not.

As last remark for this section, we just note that what has been done for the mean field analysis of the two species TASEP can straightforwardly be

extended to an arbitrary number n of species, with hopping rates $\{h_i\}_{i=1...n}$, each of them having an entrance rate given by αp_i (with, of course, $\sum_i p_i = 1$): what one obtains is a standard TASEP with effective hopping rate $h_{\text{eff}} = \sum_i p_i h_i$.

1.4 Monte Carlo Simulations

In the previous section, we analyzed our two species TASEP in the mean field approximation and we obtained the phase diagram shown in Figure 1.4. In order to be able to tell how good this approximation is and, consequently, how accurate the results obtained are, we have written a program in C++ to simulate our model. In particular, in our simulations we used the Gillespie Algorithm [14] to implement the update rule of the lattice state, so that the obtained stochastic evolution is exact and doesn't suffer any time discretization issue.

In order to better understand why we chose to use this algorithm and how it works, it is useful to revisit some basic theory about Poisson processes.

1.4.1 Poisson Stepper

The easiest Poisson process one can think of is the so called *Poisson stepper*, which is sketched in Figure 1.5: a particle moving on a 1D lattice and allowed to hop only forward to the next lattice site. In particular, the hopping process is stochastic, and the particle hops forward with rate ν, meaning that the probability that a jump event occurs in a infinitesimal time interval dt is given by νdt, with at most one event taking place at any given time interval $[t, t + dt]$. Finally, a definying and very important property of a Poisson process is that the stochastic events (in this case the jumps) are, by assumption, statistically independent.

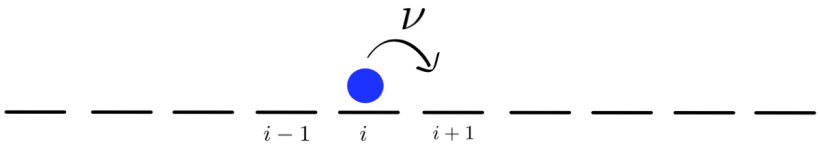

Figure 1.5: Sketch of a Poisson stepper on a 1D lattice with hopping rate ν.

From these properties of the Poisson stepper, it is relatively straightforward to derive the probability distribution of a very important observable

related to the process, namely the waiting time distribution, the distribution, i.e, of the time that one has to wait before an event occurs. In order to derive it, let's call T the waiting time between two successive events and $S(t)$ the probability that $T > t$. Then we will have that:

$$S(t) = \int_t^\infty p(t')dt' \;\Rightarrow\; p(T) = -\frac{dS(T)}{dT} \tag{1.18}$$

where $p(T)$ is the quantity that we want to compute: the probability distribution of T. Now, thanks to the statistical independece of the events assumed for the process, we can easily derive a differential equation for $S(t)$:

$$\begin{aligned} S(t+dt) &= \text{Prob}\{T > t+dt\} \\ &= \text{Prob}\{T > t\}\text{Prob}\{\text{No events in } (T, T+dt]\} \\ &= S(t)(1-\nu dt) \end{aligned} \tag{1.19}$$

where, from the first to second line we used the assumed independence of different events, while from the second to the third just the defining property of our Poisson stepper. If now we rewrite $S(t+dt)$ as $S(t+dt) = S(t)+S'(t)dt$, we obtain a differential equation for S, from which we can easily derive $S(t)$:

$$S'(t) = -\nu S(t) \;\Rightarrow\; S(t) = e^{-\nu t} \tag{1.20}$$

where we have implicitely set $S(0) = 1$, which just means that we assume that, at time $t = 0$, the stepper has not yet jumped. Having the explicit expression of $S(t)$, we can finally write $p(T)$, using the relation (1.18):

$$p(T) = \nu e^{-\nu T} \tag{1.21}$$

which is the well known exponential distribution for the waiting time of a Poisson process, and which will turn out to be extremely useful as one wants to simulate numerically such a process.

1.4.2 Gillespie Algorithm

In order to numerically simulate a Poisson process as the one described in the previous section, one could proceed in different ways. One possibility could be, for example, to divide the total simulation time in small intervals Δt, and for every interval draw a binary random variable with probability for its two outcomes of, respectively, $p_0 = \nu\Delta t$ and $p_1 = 1 - p_0$, to decide whether or not an event should occur in that time interval. In order for this approach to give accurate results, though, one needs to set $\Delta t \ll \nu^{-1}$ since, by definition

of the process, at most one event can occurr in a time interval dt. This leads to a big waste of computing time during which nothing happens ($p_0 \ll 1$), or to unaccurate and inexact results, if Δt is not chosen small enough.

Another, more clever way to proceed is by exploiting the waiting time distribution (1.20) that we found above. One could, in fact, draw a random variable which is distributed according to (1.20) and then update the system according to the result. In this way, the stochastic evolution of the system is *exact* – given, of course, that the random variable is properly distributed – and the system *moves* at every update. This is exaclty the idea behind the Gillespie algorithm, described in his original paper [14].

Practically, all that is needed is a uniform random variable generator. Given a random variable η uniformely distributed between 0 and 1, in fact, it is possible to obtain a random variable ζ distributed according to a generic distribution $p(\zeta)$: we can impose that the probability for η to be in $[\eta, \eta + d\eta]$ is the same as the one of ζ to be in $[\zeta, \zeta + d\zeta]$:

$$p(\zeta)d\zeta = 1d\eta \;\Rightarrow\; \frac{d\eta}{d\zeta} = p(\zeta) \tag{1.22}$$

So that, if we now identify ζ with the waiting time T and $p(\zeta)$ with $p(T)$ given by (1.20), we find how to obtain T from the uniform variable η:

$$\eta = 1 - e^{-\nu T} \;\Rightarrow\; T = -\frac{\ln(1-\eta)}{\nu} = -\frac{\ln \eta'}{\nu} \tag{1.23}$$

for a new uniform random variable η'.

1.4.3 The general case

The simple Poisson process described above can easily be generalized. Let $\mathcal{S}$ be a system with a discrete configuration space, and let $\{\mathcal{C}_i\}_{i=1\ldots N}$ be the N different possible configurations of $\mathcal{S}$. At every time t the system can jump in a Poisson fashion to the configuration $\mathcal{C}_i$ with rate $\mu_i(t)$, meaning that the probability for the system to change configuration in the time interval $[t, t + dt]$ will be given by: $\left(\sum_i \mu_i(t)\right) dt$, while the conditional probability that the new system configuration will be $\mathcal{C}_j$, knowing that the system has jumped, is given by:

$$p_j = \mu_j(t) \left(\sum_i \mu_i(t) \right)^{-1} \tag{1.24}$$

Within this set up, it is straightforward to generalize what has been said in the previous section, in order to simulate numerically the stochastic

evolution of such a system. In this case, the waiting time distribution will be given by:

$$p(T) = \mu(T) \exp\left\{ - \int_{t_0}^{t} \mu(T) dt \right\} \tag{1.25}$$

while the relation (1.23) becomes:

$$\ln(1-\eta) = - \int_{t_0}^{T} \mu(t) dt \tag{1.26}$$

where we have implicitely defined $\mu(t) := \sum_i \mu_i(t)$. So that to update the system we just have to draw a uniformely distributed random variable, convert it into a waiting time value using (1.26), and then, by means of another uniformely distributed random variable, decide in which of the allowed configurations the system will evolve. This last step is simply achieved: the range of the second uniform random variable is divided in N sections so that the lenght of the i-th secton is proproional to $\mu_i(t)$. In this way, the probability that the drawn value of the uniform random variable will be in the i-th section is exactly the one given by (1.24).

1.4.4 Simulating the heterogeneous TASEP

The formalism developed in the last subsection can be exploited also to implement a numeric simulation of our heterogeneous TASEP. As reminded before, in fact, the TASEP – as well as the TASEP coupled with LK and the heterogeneous versions of them – is a Markov process, meaning that the state of the system at time $t + dt$ depends only on its state at time t, and not on the state at previous times: the system has no memory and the stochastic events (i.e. the system jumping in a new configuration) can be regarded as statistically independent. Thanks to this property, therefore, we can describe our system as done in the previous section, where the configurations $\{\mathcal{C}_i\}_{i=1\ldots 3^N}$ are all the possible configurations of the lattice, while, for what concerns the rates $\mu_i(t)$, in this case they do not depend on time but only on the current configuration of the lattice, so that they are better rewitten as: $\{\mu_{ij}\}_{i,j=1\ldots 3^N}$, with μ_{ij} being the probability per unit time of jumping to the i-th configuration, given that the system is in the j-th one. With this notation equation (1.26) simplifies and can be written explicitely:

$$T_j = -\frac{\ln(1-\eta)}{\mu_j} \tag{1.27}$$

where T_j is the time one has to wait before the system jumps in a new configuration, given that it is in the j-th one, while μ_j is given by $\mu_j = \sum_i \mu_{ij}$

and η is a uniformely distributed random variable. This is precisely the setup that we used to write the program to simulate the evolution of our system.

In practice, we defined a class *lattice* containing information about the various parameters of the system ($N,\ \alpha,\ \beta,\ q,\ p$, and, for later use, the LK parameters ω_s) as well as the configuration $\mathcal{C}_j$ of the lattice (which site is occupied and by which species of particle). As auxiliary private members, we also had the total number of occupied sites, of empty sites and the total number of what we called *blocks*, namely occupied sites followed by an empty one (i.e. number of particles that may jump forward in the following step): this variables, together with the occupation state of the first and the last sites, are used to compute the total rate μ_j of the current lattice configuration $\mathcal{C}_j$. The total rate μ_j is also stored as a private member of the class. In order to make an instance of the class (i.e. a given lattice) evolve, we defined a method which updates the state of the lattice according to the Gillespie algorithm: a uniform random variable η is drawn and is converted in a waiting time T using the relation (1.27), where μ_j is the private member of the object. At this point, knowing the total number of occupied sites, of empty sites, of blocks, and the state of the first and last sites, we know how many states the lattice could evolve into, and knowing the various parameters of the model, we also know the relative probability of each of these configurations. Using a newly drawn uniform random variable, therefore, and applying the method described in the previous subsection, we decide what should happen: either a new particle enters the lattice (if the first site is empty) or a particle leaves it (if this can happen), or a particle jumps forward. If this last event is the chosen one, using another uniformely distributed random variable, we decide which one of the available particles will jump forward. Once this decision has been done, the state of the lattice, as well as all the other private members of the object, are updated consequently. Eventually, the method returns the waiting time T that has taken the system to evolve, so that it can be used to monitor the total evolution time.

To compute the average steady state densities and current, we exploited the fact that, in the stationary state, it is equivalent to sample time-wise or ensemble-wise, under the assumption that the system does not get stuck in a state for a time which is comparable with the simulation lenght. Altough nothing guarantees a priori that this is a safe assumption to make, at no point in our simulations we had reason to question the validity of our sampling method.

We started from an empty lattice and made the system evolve till it reaches a state close enough to stationarity and then sampled at equally spaced times. Since it is not clear, a priori, how much time the system needs to get close to the steady state, we first simulated the system setting both

hopping rates to 1, so that we could exploit the fact that the properties of the standard TASEP at the steady state are well known to evaluate a reasonable time $T^*_{q=1}$ from when to start the sampling. For the general case, we then set $T^*_{q<1} = T^*_{q=1} q^{-1}$, given that in the case $q < 1$, time scales have to be rescaled by q^{-1}. This choice for $T^*_{q<1}$ has proven to be a good one, since the results of the simulations have not shown significant changes upon using a consistently increased starting sampling time.

1.4.5 Simulations results

Having a program that simulates the stochastis evolution of the system, the first thing that we checked was how the total density θ (which, according to the equations (1.14), should be constant in the bulk) changes in the expected LD and HD phase upon varying, respectively, α and β, and its behaviour at the interface between these regions of the $\alpha\beta$ plane and the MC one.

In order to do this, we started by looking at what happens around values of α and β corresponding to values for the effective parameters (1.15) of $\alpha^* = 1/2$ and $\beta^* = 1/2$. The results of these first simulations are shown in the two plots of Figure 1.6, for a fixed choice of p and q. What we observe

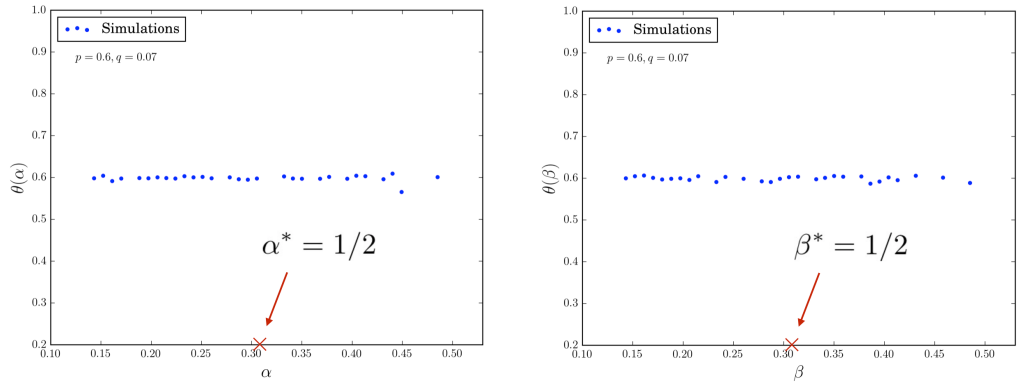

(a) (b)

Figure 1.6: Simulation results for θ as a function of α in a neighborhood of $\alpha^* = 1/2$ (a) and as a function of β in a neighborhood of $\beta^* = 1/2$ (b). Both plots show a constant behaviour of the total density θ across the scanned values of α and β. This suggests that, for these values of the entrance and exit parameters, the system is in a MC-like phase and does not exhibit the transitions predicted by the mean field theory.

in these plots is that the total density θ is constant - modulo some obvious fluctuations - upon varying α and β, both above and below $\alpha^* = 1/2$ and

$\beta^* = 1/2$. Moreover, we notice that this constant value is not compatible with the expected one of $\theta = 1/2$ in the MC phase (Eq. (1.14)) – the only one where a constant total density is expected. This tells us that the mean field approximation is probably not as accurate as we hoped.

After these first findings, we explored the phase space further, and finally found regions where the total density is no longer constant but, rather, depending on α or β, in a similar fashion to what one would expect in the predicted LD and HD phases. Moreover, we recovered the continuous transitions between these phases and the previously discovered constant density phase (which, from now on, will be referred to as the MC phase). These findings are shown in Figures 1.7 and 1.8.

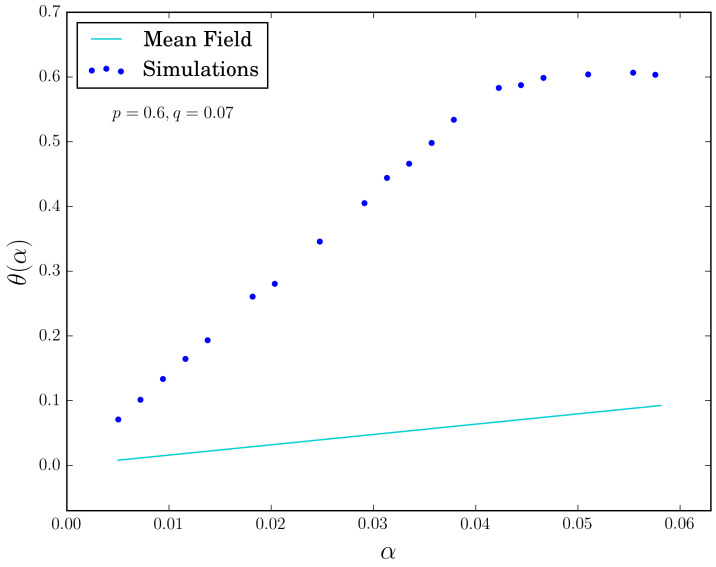

Figure 1.7: Simulations data for the total density as a function of α (scattered points) at the boundary between two phases, plotted against the mean field prediction (continuous line). The plot shows a continuous phase transition between a LD-like phase, where the density grows with the entrance paramenter α, and the previously discovered MC phase where the total density, for the particular choice of p and q, assumes a constant value of $\theta \approx 0.6$. This transition is qualitatively the same as the one predicted by the mean field theory, but, as can be seen here, it happens at a much lower value of α.

From these plots we see that the qualitative behaviour is exactly the one given by the phase diagram in Figure 1.4, but the critical values of α and β

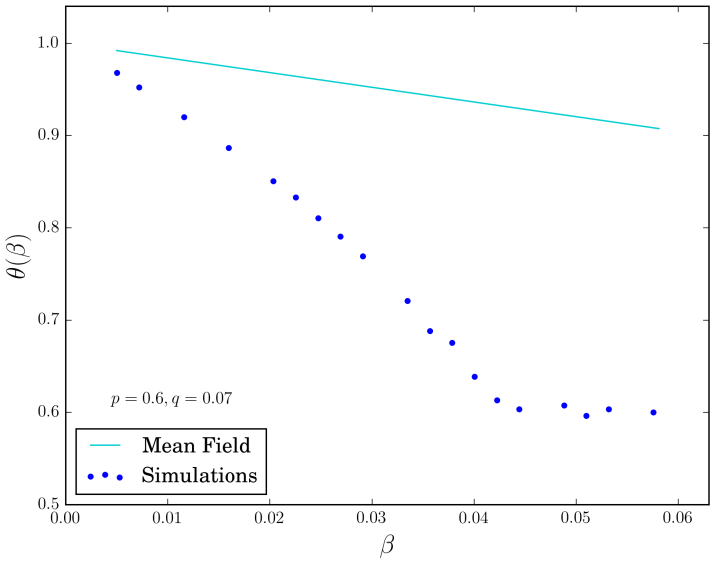

Figure 1.8: Simulations data for the total density as a function of β (scattered points) at the boundary between two phases, plotted against the mean field prediction (continuous line). As in Figure 1.7, also this plot shows a continuous phase transition, this time between a HD-like phase, with a density dependence on β, and the MC phase. Again, this transition is qualitatively the same as the one predicted by the mean field theory, but, as can be seen here, it happens at a much lower value of β.

at which the transition between the LD and HD phases and the MC one are completely different from the ones predicted by the mean field analysis, as well as the value of the total densities in these three different phases.

As last thing, we also checked the expected avarage current in the bulk as a function of θ (equation (1.16)) against the simulations, and – at this point not with surprise – we found that, also for this quantity, the mean field predictions are by no means in agreement with the simulations, as it is shown in the plot in Figure 1.9.

As it is clear, the simulations that we performed show that the results obtained by the mean field approximation cannot be regarded as a good description of our system at the steady state. Therefore, in the next chapter we will try to develop a more accurate theory which goes beyond the simple mean field one.

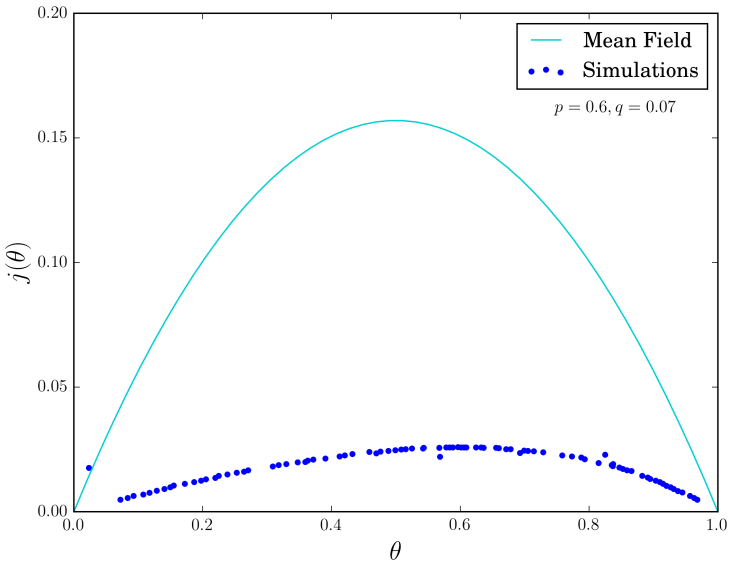

Figure 1.9: Here the simulation results for the average bulk current as a function of the total density θ are plotted against the theoretical values obtained by means of the mean field analysis (1.16). The true value of the average current turns out to be much lower than the one that the mean field theory predicted, showing that the reduced hopping rate q heavily influences the mobility along the lattice. Moreover, we also see that, while the mean field current-density relation is symmetric in θ, the true relation is not, so that the MC phase density – as we found out above – is no longer given by $\theta_{MC} = 1/2$, but, rather, assumes an higher value.

Chapter 2

Refined Mean Field Theory

As we saw in the last chapter, a simple mean field approximation doesn't provide a satisfying description for the stationary state of our model. Therefore it is necessary to develop a more refined approximation, in order to get results which are in better agreement with the simulations.

First of all, we have to identify the reason why the mean field analysis has failed. Intuitively, this could be traced back to the fact that, having particles that hop at very different rates, some jamming phenomena will emerge, where fast particles will accumulate beyond a slow one, so that correlations between the positions of particles cannot really be neglected. This idea is also supported by the kymographs that we obtained from the simulations, an example of which can be seen in Figure 2.1.

These kymographs show how, under the right conditions, the heterogeneous TASEP process that we are considering appears made of clusters, rather than single particles, which moves to the right with a rate proportional to the smaller hopping rate q – where, with *clusters*, we refer to the ensemble of one slow particle and the fast ones that accumulate behind it.

These findings suggested the idea to try to map our heterogeneous TASEP to a standard TASEP where particles have a finite size d and occupy more than one lattice site. However, in our case, the clusters won't have all the same size (which is nothing else than the number of the fast particles in the cluster plus one slow particle). We decided, therefore, to use, as a first approximation for the particles size d, the average lenght of a cluster. This is easily computed as follows (see also Fig. 2.2):

$$\langle l \rangle = 1 + \sum_{d=0}^{\infty} d(1-p)p^d = \frac{1}{1-p} \tag{2.1}$$

For a cluster of lenght d to enter the system, in fact, a slow particle must

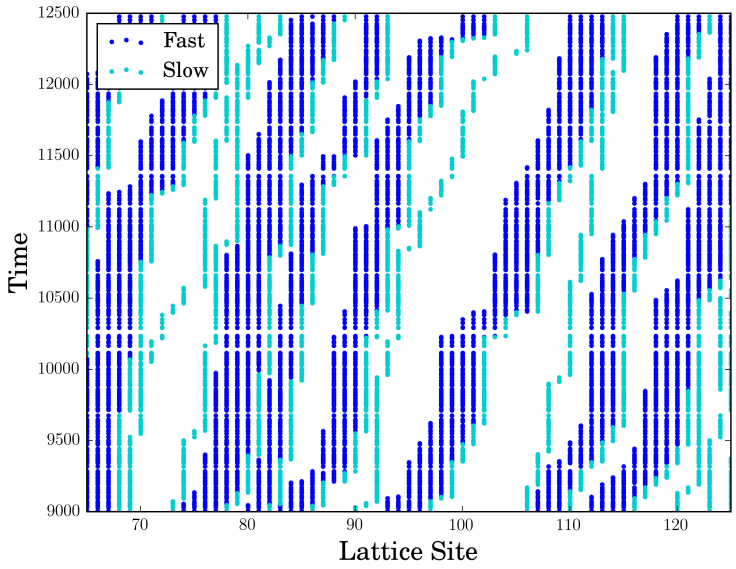

Figure 2.1: Section of a simulated kymograph for the system close to the steady state, for given q and p. Here we can see the jamming of fast particles (blue points) behind a slow one (light blue). This give rise to a system which seems to be made of clusters wich move forward with average velocity of the order of q (the proceeding of non-empty clusters, in fact, is similar to the one of empty ones, i.e. single particles of the second species).

first enter and then we need that other $d-1$ fast particles enter the lattice after that one, and before the next slow one. And since these elementary events are independent by assumption, the probability of the whole event to happen is given by $(1-p)p^d$. The 1 is then added to take into account the *empty* clusters, the ones, i.e., consisting only of a slow particle.

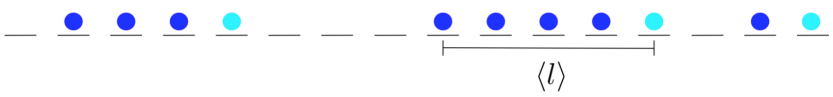

Figure 2.2: Example of a lattice section, with clusters of different sizes

As last remark, we note that, for the finite size particles TASEP approximation to be consistent, we need to impose some contraints on the hopping rate q and the relative fraction of fast particles p. We want, in fact, our clusters to behave as closely as possible to rigid particles of lenght $\langle l \rangle$. How-

ever, they are not single bodies: once the slow particle at the right end of one cluster hops forward, a hole is created inside that cluster, and if the slow particle cap hops forward again before that hole has travelled all the way left and exited the cluster, then we will have two holes, and so on if this happens again. And it is clear that the more holes in the cluster, the less appropriate our description of it as a single particle of definite size will be. We decided, therefore, to constraint the parameters q and p so that at most one hole at the time is present in each cluster. This is done by requiring the avarage time that the slow particle at the right end takes to hop forward to be much bigger than the avarage time needed by the hole to exit the cluster. These two quantities are given, respectively, by q^{-1} and $\langle l \rangle - 1$. So that, in the following, we will be imposing:

$$\frac{1}{q} \gg \langle l \rangle - 1 \quad \Rightarrow \quad \frac{qp}{1-p} \ll 1 \tag{2.2}$$

2.1 Refined MF analysis for the current

We will now apply the ideas explained in the previous section to derive a more accurate expression for the steady state current and, from it, obtain expressions for the densities. In particular, the total average current between the site i-th and the $(i+1)$-th one is given by $j_i = j_\rho^i + j_\mu^i$, where j_ρ^i is the contribution to the average current given by the fast particles, while j_μ^i the one given by the slow ones. So that, we can analyze these two contributions separately. We will start with the average current associated with the slower particles: j_μ^i.

2.1.1 Slow particles

We start analyzing the contribution to the current due to the slow paticles. The quantity that we need to compute is:

$$j_\mu^i = qP\{m_{i+1} = n_{i+1} = 0 | m_i = 1\} P\{m_i = 1\} \tag{2.3}$$

where the second factor is nothing else than the density μ_i itself ($\mu_i = 1(P\{m_i = 1\}) + 0(P\{m_i = 0\})$), while the first one is the conditional probability that the $(i+1)$-th site is empty given that the i-th site is occupied by a slow particle. It gives, therefore, the fraction of slow particles which are free to jump forward. This is the term where correlations come into play. Hence, let's now focus on it.

As we explained above, as long as the condition given by (2.2) is satisfied, we can think of the system as being made of clusters of an avarage lenght $\langle l \rangle$

whose right tips consist of slow particles, and that have at most one hole in them. We can therefore, map this model to a TASEP with particles of finite size $\langle l \rangle$ and hopping rate given by q.

Such problem has been treated in detail by Lakatos and Chuo in [15]. In this work, in fact, the authors found that a simple mean field analysis fails also in the case of a standard TASEP with extended particles and, therefore, they derived a more accurate approximation for a TASEP with particles of size $d > 1$ and hopping rate $h = 1$. In particular, analysing the system in the Maximal Current Phase, they found the following expression for the avarage current in the stationary state:

$$j_d(\sigma) = \sigma \frac{1 - \sigma d}{1 - \sigma(d-1)} \tag{2.4}$$

where σ is their particle density and d the size of the particles.

If we now replace d with the avarage lenght of our clusters $\langle l \rangle$, σ with μ, and divide by μ (in order to isolate the first factor on the RHS of equation (2.3)), we obtain the following expression for the fraction of slow particles free to hop forward:

$$f_p(\mu) := P\{m_{i+1} = n_{i+1} = 0 | m_i = 1\} = \frac{1 - \mu \langle l \rangle}{1 - \mu(\langle l \rangle - 1)} \tag{2.5}$$

where the subscript p makes explicit the dependence on the fraction of fast particles, encoded in the avarage lenght $\langle l \rangle$. With this quantity at hand, it is now straightfoward to write down the approximate slow particles current: keeping in mind that for us the hopping rate is given by $q < 1$, we have:

$$j^{\mu}_{p,q}(\mu) \approx q f_p(\mu) \mu \tag{2.6}$$

2.1.2 Fast particles

Let's now consider the current associated to the fast particles. We want to compute the $\rho-$current at the i-th site, which is again given by:

$$j^i_{\rho} = P\{m_{i+1} = n_{i+1} = 0 | n_i = 1\} P\{n_i = 1\} \tag{2.7}$$

where, as before, n_i and m_i are, respectively, the number of fast and slow particles at site i. Exactly as before, the second factor of the right hand side of (2.7) is nothing else than the density, ρ_i, while the first is the most interesting and less trivial one, and the one that we have to find a good approximation for. The good news is that, under the assumption that, in

each cluster, there is, at most, one hole at the time, computing this quantity is not too complicated, as it will become clear in the following.

In such regime, in fact, given a closed cluster of lenght $\langle l \rangle$ – which means one slow particle followed by $\langle l \rangle - 1$ fast ones – we know that it will become open (namely, that the slow particle at the rightmost end of the cluster will jump forward, so that a hole will enter the cluster) on average every $(qf_p(\theta))^{-1}$ time units (we have implicitely assumed that at each slow particle corresponds a cluster, and used the result according to which only a fraction $f_p(\mu)$ of them is free to jump forward). So, the first fast particle of the cluster will be free to move, on average, every $(qf_p(\theta))^{-1}$ time units. The second one has to wait until also the first fast particle of the cluster has jumped, so that it will be free to move on avarage every $(qf_p(\theta))^{-1} + 1$ time units, the third one only every $(qf_p(\theta))^{-1} + 2$ time units, and so on, till the last one, which, on average, will be free to jump forward every $(qf_p(\theta))^{-1} + \langle l \rangle - 2$ time units. Averaging over the whole cluster, we find the following approximation for our probability:

$$\begin{aligned}[P\{m_{i+1} = n_{i+1} = 0 | n_i = 1\}]^{-1} \approx \frac{1}{\langle l \rangle - 1} \sum_{i=0}^{\langle l \rangle - 2} \left(\frac{1}{qf_p(\mu)} + i \right) = \\ = \frac{2 + qf_p(\mu)(\langle l \rangle - 2)}{2qf_p(\mu)}\end{aligned} \tag{2.8}$$

We can now use this result to write a refined expression for the current due to the fast particles (2.7):

$$j^{\rho}_{p,q}(\rho, \mu) \approx \frac{2qf_p(\mu)}{2 + qf_p(\mu)(\langle l \rangle - 2)} \rho \tag{2.9}$$

2.1.3 On the degrees of freedom

In the first chapter, we had proven the relations (1.12), which allowed us to obtain the local densities ρ_i and μ_i from the total density θ_i and which, de facto, reduced the number of degrees of freedom of the problem, allowing us to concentrate only on the total density.

Unfortunately, this very useful result holds exactly only in the mean field limit, and, as we saw in the section on Monte Carlo Simulations, this limit does not accurately describe our system. However, since the relations (1.12) would simplify our problem considerably, it would be of great help if they held to some extent in the case of the heterogenous TASEP.

As already explained before, thanks to particle conservation in the bulk, global relations of the kind of (1.12) always hold for the average total number of particles, even if correlations cannot be neglected. For this reason, if the density happens to be constant along the lattice, then one can straightfowardly argue that (1.12) hold also in their local form.

We therefore ran some more simulations for different values of the parameters α and β, to check whether or not the system at stationariety shows constant density profiles. The results of these simulation are shown in Figure 2.3. From these plots we can see that, a part from the regions near the tips,

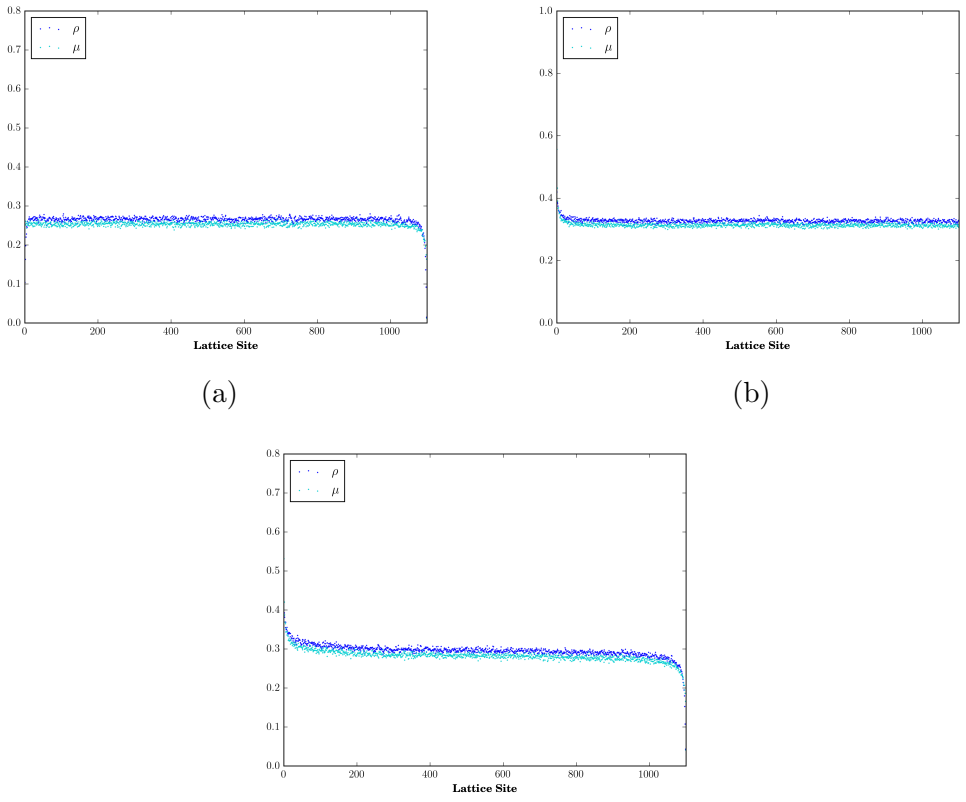

Figure 2.3: Simulation data of the density profiles of the two species of particle, for a lattice of lenght $N = 1100$, and with $p = 0.51$ and $q = 0.07$, for different values of the entrance and exit parameters: (a) $\alpha = 0.037$ and $\beta = 1$. (b) $\alpha = 1$ and $\beta = 0.037$. (c) $\alpha = 0.3$ and $\beta = 0.3$. In all three cases we witness a constant average density in the bulk for both species of particles.

the average densities of both species of particles remain constant along the lattice, so that, according to what has just been said, we can argue that it is safe to consider the relations (1.12) valid also in the heterogeneous TASEP case.

Using the relations (1.12) and the expressions found previously for $j_{p,q}(\rho)$ and $j_{p,q}(\mu)$, we can, therefore, write the refined mean field version for the avarage current as a function of the total density θ:

$$j^{tot}_{p,q}(\theta) \approx \left[(1-p)qf_p(\theta) + p\frac{2qf_p(\theta)}{2+qf_p(\theta)(\langle l\rangle - 2)}\right]\theta \tag{2.10}$$

where $f_p(\theta)$ is given by $f_p(\theta) := f_p(\mu)|_{\mu=(1-p)\theta} = \frac{1-\theta}{1-p\theta}$.

We can now finally test this result against the simulations, to check whether or not the refined mean field analysis that we developed so far represents a better description of the system. In Figure 2.4, therefore, we plot the same simulation data as in Figure 1.9 against the theoretical current given by (2.10).

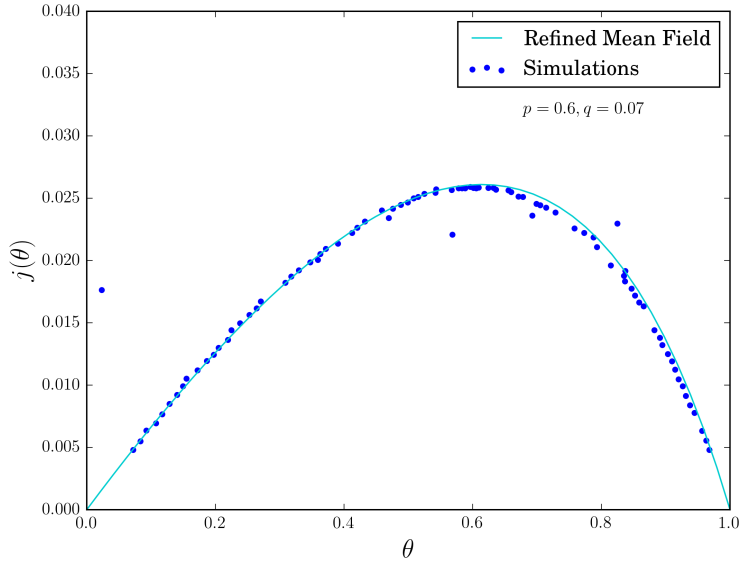

Figure 2.4: Comparison between simulations and refined mean field theory for the avarage bulk current as a function of the total density θ. We note that with the refined mean field expression for the current (2.10) we obtain a much better agreement than with the simple mean field one, including the asymmetric relation between θ and j.

2.2 Refined mean field analysis for the densities

Having found an approximate expression for the current-density relation which is in good agreement with the simulations, (2.10), we can now use it to derive an approximation for the total density in the Maximal Current phase, and then match it to the Low Density and High density phases.

2.2.1 Maximal Current Phase

In order to get the value of the total density θ in the Maximal Current Phase, we need to find the value of θ that maximises the current in equation (2.10). To this end, we computed the derivative of $j^{tot}_{p,q}(\theta)$ with respect to θ and then fed the result to Mathematica to obtain its zeroes.

Unfortunately, the expressions that one gets as an answer, being several pages long, are of no practical use, and don't convey any intuition. We thought, therefore, that, since for $q \to 1$ we recover the behaviour of the standard TASEP, the most interesting regime is the one for low hopping rates and, consequently, it makes sense to try to make the results tractable by expanding them for small hopping rates q.

This approach simplifies things immensely. At first order in q, in fact, the derivative with respect to θ of the current (2.10) reads:

$$\partial_\theta j^{tot}_{p,q}(\theta) = \frac{1 - 2\theta + p\theta^2}{(p\theta - 1)^2} q + o(q^2) \tag{2.11}$$

whose zeroes in θ are easily found:

$$\theta_1 = \frac{1 - \sqrt{1-p}}{p} \quad \wedge \quad \theta_2 = \frac{1 + \sqrt{1-p}}{p} \tag{2.12}$$

Of these two candidate values for the Maximal Current density, only the first one, θ_1, is a sensible choice, since the second one is always bigger than 1, which the density cannot be. So that the refined mean field value of the density in the Maximal Current phase is given by:

$$\theta_{MC} = \frac{1 - \sqrt{1-p}}{p} \tag{2.13}$$

Firstly, we notice that this density does not depend on q, as one would expect intuitively, given that for $q \to 1$ one recovers the standard TASEP and, therefore, a MC phase density of $\theta_{MC} = 1/2$, as it is also shown in Figure 2.5(b). This can be justified if we remember that the expression (2.13) has

been obtained in the limit $q \to 0$ and, therefore, it should be regarded as valid only in a small neighborhood of $q = 0$.

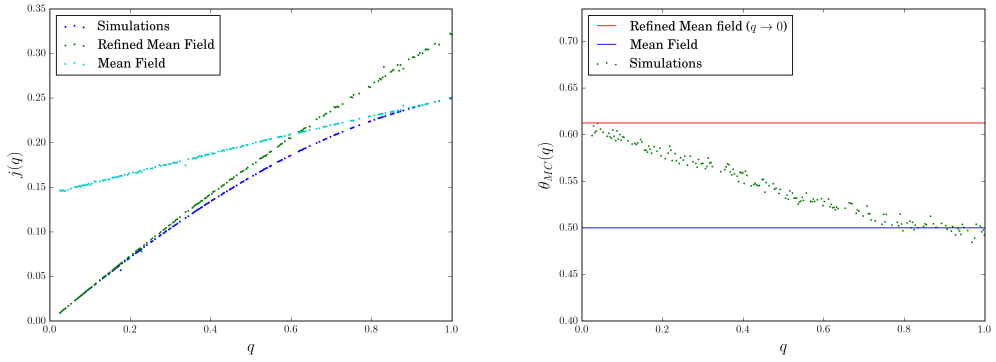

(a) (b)

Figure 2.5: (a) Simulation data for the maximal current value in the bulk as a function of q, plotted against the mean field and the refined mean field predictions for a fixed value of $p = 0.6$ (To compute these values, the simulated total density θ has been plugged in in the equations (1.16) and (2.10)). We see that our mean field theory works very well for low q, as expected from (2.2), while for $q \to 1$, we recover a good agreement with the mean field theory and a current that asymptotically reaches the standard value of $j_{MC} = 1/4$. (b) Here the MC phase density is plotted as a function of the hopping rate q, for the same fixed value of p as in (a). Again we see that for very small q, the simulations agree with our theory, as we expected, while, as q grows, the MC density decrease till the mean field value of $\theta_{MC} = 1/2$.

Secondly, we also note that, for $p \to 1$, the density (2.13) does not approach the Maximal Current density of the standard TASEP, which, again, would be $\theta_{MC} = 1/2$. This discontinuity can be understood if we remember that we derived the current (2.10) under the assumption (2.2) which forces the hopping rate to go to zero with p going to one and to do so faster than p reaches this limit. As p approaches 1, therefore, the condition (2.2) forces the system extremely far from the standard TASEP, so that, in the models space, there will be a jump from the models that one gets for $p \to 1$ and the one at $p = 1$, and this justifies, at least intuitively, the discontinuity in the Maximal Current density.

2.2.2 Low Density Phase

As shown by the Monte Carlo Simulations, the Phase Diagram that we expect for our model is qualitatively the same as the one of the standard TASEP. In the previous subsection we derived an approximate expression for the avarage total density in the MC phase, and now we want to match it continously to the one in the Low Density phase.

At the light of the simulations data (see, as an example, Figure 1.7) we are brought to believe that a sensible approach - which happens to be also the easiest that one can think of - is to approximate our model in the Low Density phase as a standard TASEP with reduced hopping rate q. This appears sensible if we think that, in the Low Density phase, very few particles will be in the system, so that correlations won't be likely to play a crucial role and we can, therefore, imagine the dynamics to be determined by the slowest particles. Under this assumption, the avarage total density in the LD phase will have, therefore, the following form:

$$\theta_{LD}(\alpha) = \frac{\alpha}{q} \tag{2.14}$$

From this expression for $\theta_{LD}(\alpha)$ we can derive the critical value of the entrance parameter α at which the phase transition between LD and MC happens, i.e. that value $\tilde{\alpha}$ such that $\theta_{LD}(\tilde{\alpha}) = \theta_{MC}$. We find:

$$\tilde{\alpha} = q\theta_{MC} = \frac{1 - \sqrt{1-p}}{p} q \tag{2.15}$$

As before, we can now compare this result with our simulations. In particular, we use again the same values of p and q as in the case of the previous plots. What we obtain is showed in the plot at Figure 2.6.

This plot confirms that our ideas regarding the behaviour of the system in the LD phase were reasonable and confirms that our refined mean field theory describes the model much more accurately than the simple mean field one.

Now, the only thing left to do in order to be able to draw a complete Phase Diagram, is to study what happens in the High Density phase.

2.2.3 High Density Phase

As the last step, we now have to focus on the High Density Phase. First of all, from plots 1.7 and 1.8 (and from other similar ones that we obtained for different values of p and q), we conclude that it is safe to assume that the critical values of α and β at which the transitions between LD and MC, and

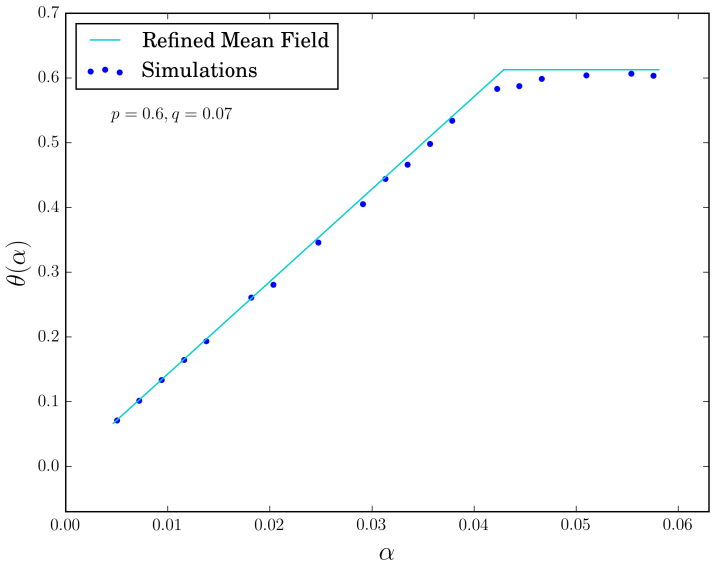

Figure 2.6: Comparison between simulations and refined mean field theory for $\theta(\alpha)$ at the interface between LD and MC. We observe that our assumption that in the LD phase is the dynamics the slow particles to shape the density profile leads to a correct prediction for the functional dependence of θ_{LD} on the entrance rate α.

between HD and MC are the same. With this information, we only need to specify the dependence on β of the HD density and then impose a continous matching with the MC density at $\beta = \tilde{\beta} = \frac{1-\sqrt{1-p}}{p} q$.

Inspired by the success obtained in the LD phase and looking at the plot in Figure 1.8, the first and simplest ansatz is a linear dependence of the total density θ on the exit parameter β:

$$\theta_{HD}(\beta) = 1 - \kappa\beta \tag{2.16}$$

where, as explained before, the constant κ is simply found by imposing continuity at the phase transition:

$$\theta_{HD}(\tilde{\beta}) = \theta_{MC} \quad \Rightarrow \quad \kappa = \frac{1 - \theta_{MC}}{\tilde{\beta}} \tag{2.17}$$

This result is, as done above for $j_{p,q}(\theta)$ and $\theta_{LD}(\alpha)$, confronted with the simulation data plotted in Figure 1.8. The plot is shown in Figure 2.7.

The first thing that we notice from this plot is that the agreement between

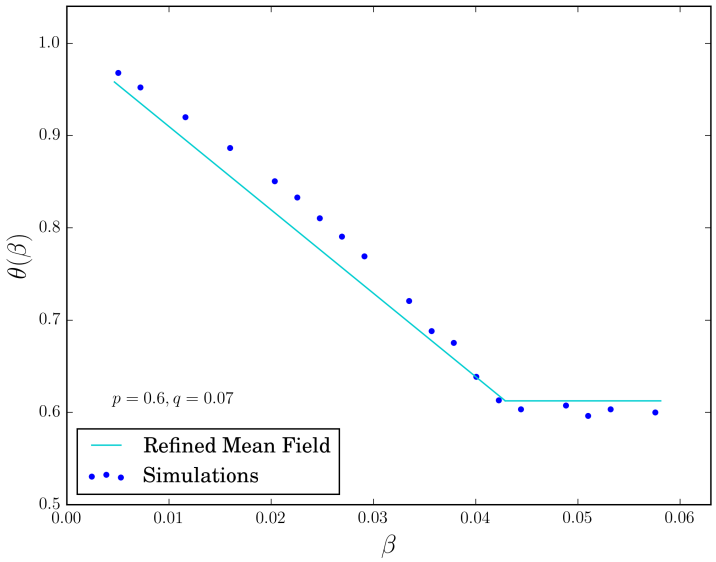

Figure 2.7: Comparison between simulations and refined mean field theory for θ at the interface between HD and MC. Conversely to what has been observed in the LD phase, here a simple linear dependence of θ_{HD} on β doesn't faithfully describe the density behaviour on varying the exit rate. This is most likely due to the fact that, in th HD phase, the lattice is extremely crowded, and the frequent interactions between slow and fast moving particles cannot be neglected and give rise to this non linear dependece.

theory and simulation is, also in this case, much better than in the case of the mean field approximation (see Figure 1.8), and that our assumption for the critical value of β at which the phase transition happens (namely that it is the same as the critical value of α for the LD-MC transition) was correct. On the other hand, we also notice that the hypotized linear dependence of θ_{HD} on the exit rate β does not seem to capture the true behaviour of the HD phase density, and – more surprisingly – that it seems to disagree also on the slope that it assumes for small values of β.

Although, at this stage, we could be satisfied with such result – being the agreement with simulations much better than the one given by the mean field approach, and being the relative error of the order of 10^{-2} – we can nonetheless make some further considerations about the density dependence on β in the HD phase.

In particular, it is easy to derive an expression for $\theta_{HD}(\beta)$ whcih is exact

in the limit of very small β. For $\beta \to 0$, in fact, we can imagine the lattice to fill up completely before the particle on the last site leaves it. And after that, once a hole has entered the system from the right, it will exit from the left (i.e. the lattice will fill up completely again) before another hole enters. More quantitively, as it is shown in Figure 2.8, once the lattice is completely filled up, it will take, on average, β^{-1} time units for a hole to enter the system and then it will take on average 1 or q^{-1} time units for the last site to become occupied again – depending on which species of particle occupies the $(N-1)$th lattice site – given that β is small enough, so that no other holes enter the system in the meantime.

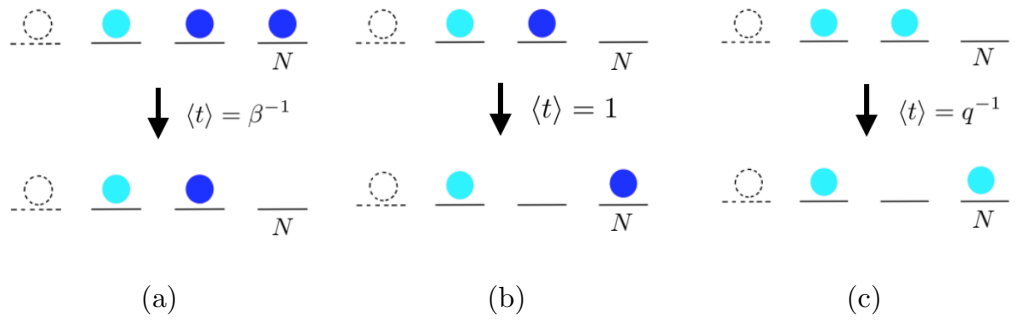

(a) (b) (c)

Figure 2.8: Average time for a hole to enter the lattice (a), and avarage times for the last lattice site to become occupied (in the limit of a full lattice) in the case of a fast particle (b) and a slow one (c).

From this consideration, we can easily compute the quantity $\theta_N(\beta)$ which is the particle density on the last site, and which will provide the value of the bulk density in the HD phase. Called $t = \beta^{-1}$ the average time during which the last site is occupied and $\tau = p + (1-p)/q$ the average time during which it is empty (where we have used the fact that we have a fraction p of particles of the first species and a fraction $(1-p)$ of the second one), we have that:

$$\theta_N(\beta) = \frac{t}{t+\tau} = \frac{q}{q+\beta(pq+1-p)} \approx 1 - \frac{pq+1-p}{q}\beta \tag{2.18}$$

where, in the last step, we used the fact that here we are considering $\beta \to 0$. As we see from this equation, in the small β regime, we recover a linear dependence of the density on the exit parameter, but with a different coefficient than the one that we obtained in the refined mean field, given by equation (2.17). As said before, in fact, this is an exact result, and in Figure 2.9, it is

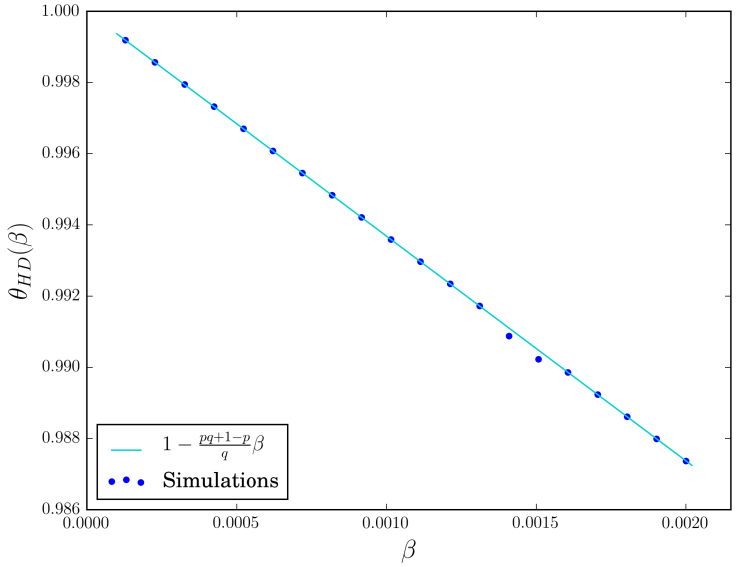

Figure 2.9: Simulation and theoretical values (equation (2.18)) of $\theta_{HD}(\beta)$ for $\beta \to 0$. As we expected, the result derived in (2.18) agrees perfectly with the simulations, sustaining the claim that, for $\beta \to 0$, this is an exact result.

plotted against the simulation data for the same values of q and p used for the plot in Figure 2.7.

For what concerns higher values of β, things are, unfortunately, not so straightforward. One possible way to go is to make an educated guess on the functional form of $\theta_{HD}(\beta)$ such that for low β the linear behaviour (2.18) is recovered, and then match it at $\tilde{\beta}$ with the MC phase density θ_{MC}.

The easiest ansatz that we could think of is a density of the form:

$$\theta_{HD}(\beta) \approx 1 - \hat{\kappa}\beta^{1+\eta\beta} \tag{2.19}$$

where $\hat{\kappa}$ is exactly the coefficient given by equation (2.18), since, for $\beta \to 0$, equation (2.19) becomes: $\theta_{HD}(\beta) = 1 - \hat{\kappa}\beta + o(\beta^2)$, whereas the factor η can be obtained by imposing that $\theta_{HD}(\tilde{\beta}) = \theta_{MC}$. This yields:

$$\eta = \left[\frac{\ln((1-\theta_{MC})/\hat{\kappa})}{\ln(\tilde{\beta})} - 1\right]\tilde{\beta}^{-1} \tag{2.20}$$

Having values for the two parameters $\hat{\kappa}$ and η that enter in the equation (2.19), we can now plot it againts the same simulation data of the plot in figure 2.7. The result is shown in Figure 2.10. From this plot we see that

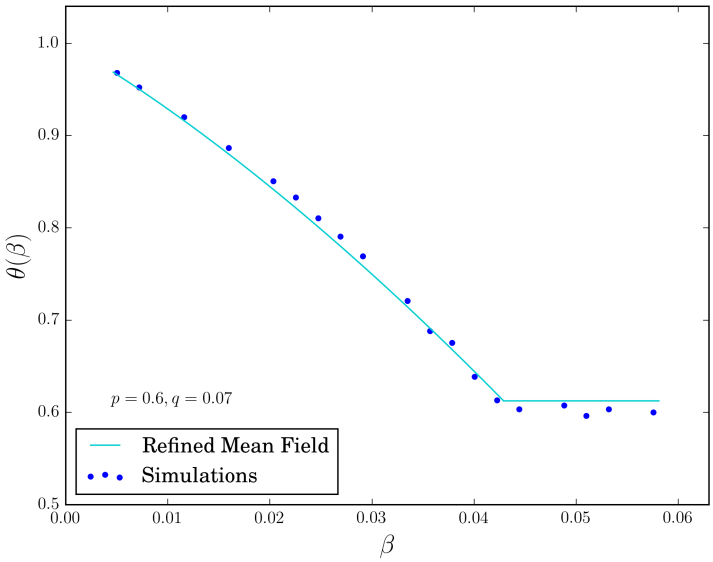

Figure 2.10: Improved density relation in the HD phase plotted against the simulation data, with $\hat{\kappa}$ and η given, respectively, by equations (2.18) and (2.20). We note that the agreement between theory and simulations is now almost perfect for low β and, also for higher values of the exit parameter, the agreement has improved with respect to the linear case of Figure 2.7.

the agreement between equation (2.19) and simulations is not only almost perfect in the small β region, as we expected, but is also much better than the linear case (Figure 2.7) for bigger values of β. Therefore, even though our intuition for equation (2.19) is not as good as for the very small β regime, we decided to keep this functional dependence for $\theta_{HD}(\beta)$.

2.2.4 The Phase Diagram

Now, we can finally combine the results found so far to draw the Phase diagram of our model in the steady state. The result is shown in Figure 2.11.

What we have obtained is a Phase Diagram qualitatively identical to the one given by the mean field theory, but with quantitative values for the densities and the critical values of the parameters that are in much better agreement with the simulations, as shown above.

In particular, under the condition (2.2) and for small hopping rate q, we recover a phases diagram characterized, as for the standard TASEP, by three different phases, in which the avarage total density θ assumes the following

values:

$$\theta_{LD}(\alpha) = \frac{\alpha}{q}$$

$$\theta_{MC} = \frac{1 - \sqrt{1-p}}{p} \tag{2.21}$$

$$\theta_{HD}(\beta) = 1 - \frac{pq + 1 - p}{q}\beta^{1+\eta\beta}$$

with η given by equation (2.20).

As an example, in Figure 2.12, we plotted the density profiles in the three phases for a particular choice of α, β, p and q. As we can see, a part from boundary effects due to the finite size of the system (here $N = 1100$), the agreement between our Refined Mean Field theory and the simulation is, as expected, much better than in the simple Mean Field case.

2.2.5 Boundary effects

For what concerns the boundaries, the discrepancies between the bulk density and the boundary one in the rightmost part of the lattice in the LD phase, in the leftmost part of the lattice in the HD phase, and on both sides of the lattice in the MC phase, can be explained in complete analogy to the standard TASEP, where such effects are also present (see, for example, [9] and [16], or [13]). Briefely, What happens in the standard TASEP is that, at the boundaries, the value of the density is determined by the *reservoirs* densities – namely $\theta = \alpha$ on the left and $\theta = 1 - \beta$ on the right. In the LD phase is the left boundary which dictates the density along the whole lattice, while in the HD phase is the right boundary the one which drives the transition and imposes its density value. This leads to boundary layers to arise on the left or on the right, respectively in the HD and in the LD phase, because, at the boundaries, the density is bounded to the reservoir's one, while, in the bulk, it is dedermined by the opposite lattice end. In the MC phase, on the other hand, the bulk density is neither the left or the right one, so that boundary layers appear on both ends of the lattice.

From the plots in Figure 2.12, we see that this phenomenon appears, as one would expect, in our case as well. One interesting and new phenomenon, though, is present here, which, at first, does not seem to be in agreement with the behaviour of the standard TASEP. If we zoom-in on the left tip of the lattice in the LD phase (see Figure 2.13(a)), in fact, we see that the fast

particle density ρ – and, therefore, the total one as well – does not remain constant till the beginning of the lattice as one would expect in the LD phase – as we explained above and as, for example, does the slow particle density – but, rather, it decays. And, as it is shown in the plots in Figure 2.13, it decays until it reaches, near the first lattice site, the left boundary density value that we would expect from a standard TASEP with hopping $h = 1$ and entrance parameter given by $p\alpha$.

This last observation gives us a hint on the reason behind this phenomenon. What seems to happen, in fact, is that, in the LD phase, near the left end of the lattice, the two species of particles ignore each other: both densities ρ and μ assume the value that they would have in a one species TASEP, namely a density of $p\alpha$ for a TASEP with hopping rate $h = 1$ and entrance rate $p\alpha$ and a density of $(1-p)\alpha q^{-1}$ for a TASEP with $h = q$ and entrance rate $(1-p)\alpha$. Then, as one moves to the right, the fast particles begin to *feel* the presence of the slow ones, and, consequently, their average velocity is reduced, so that, effectively – as we argued before in order to justify the choice of the density in the LD phase (2.14) – they behave as slow particles, and one is left with a standard TASEP with hopping rate $h_{\text{eff}} = q$ and entrance rate α.

These considerations suggest that this phenomenon is, in fact, explainable in total analogy with the boundary effects of the standard TASEP: here as well each species density is, near the first lattice site, bound to the density value of the reservoir, which is exactly $p\alpha$ for the first species and $(1-p)\alpha q^{-1}$ for the second species. As we explained above, whenever, the bulk density disagree with the reservoir value, one boundary layer does appear, and this is exactly the case for the fisrt species particle density on the left lattice end in the LD phase.

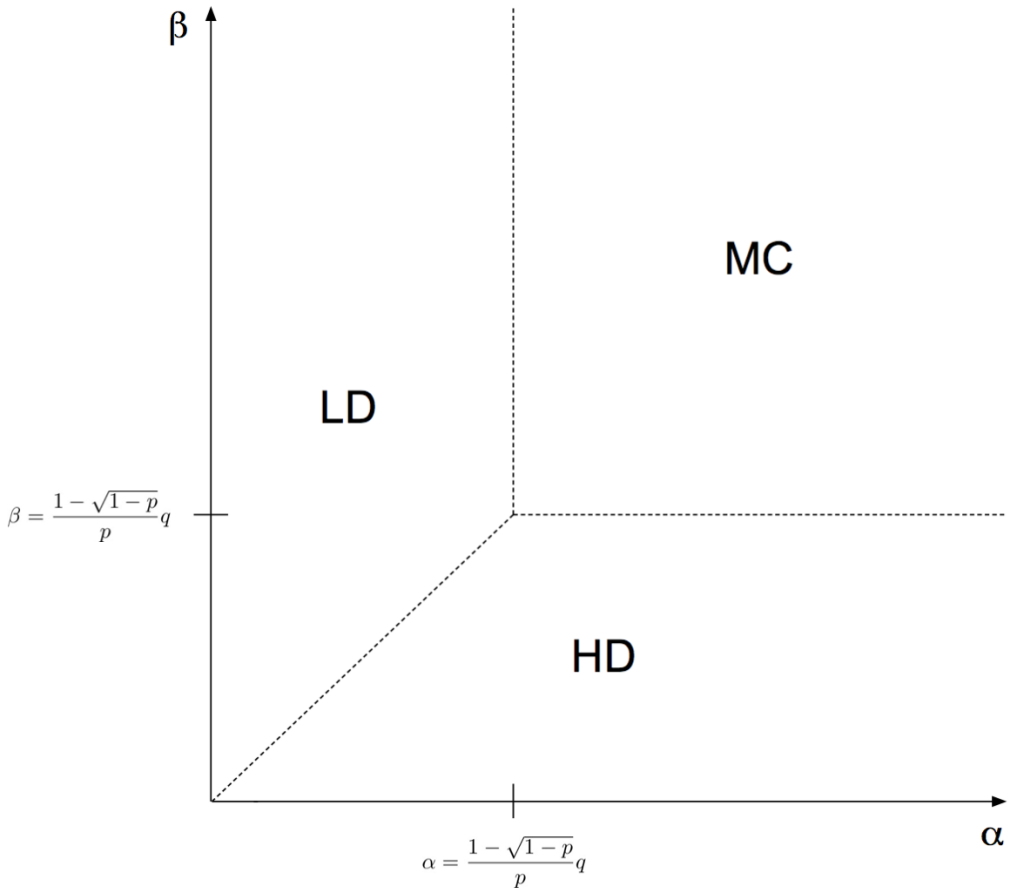

Figure 2.11: Refined mena field Phase diagram for the 2-TASEP, where the values for the bulk density in the three phases are given by equations (2.21). The qualitative structure is the same as in the standard TASEP phase diagram: a LD, a HD and a MC phase. Quantitatively, though, the transition between the phases happen at different values of the parameters from the ones predicted by the mean field theory, and the values of the bulk densities in these regions are also different from the mean filed ones.

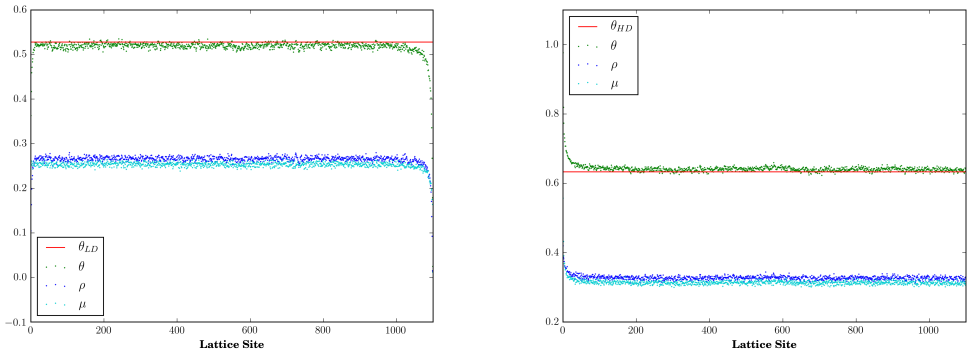

(a)

(b)

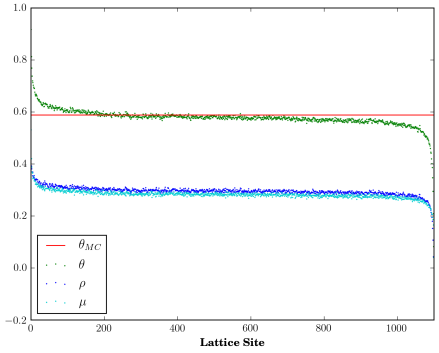

(c)

Figure 2.12: Simulation data (scattered points) of the density profiles in the three phases plotted against the refined mean field prediction for the total density θ (continous red line), for a lattice of lenght $N = 1100$, and with $p = 0.51$ and $q = 0.07$: (a) LD phase, with $\alpha = 0.037$ and $\beta = 1$. (b) HD phase, with $\alpha = 1$ and $\beta = 0.037$. (c) MC phase, with $\alpha = 0.3$ and $\beta = 0.3$. Also in this plots we notice the good agreement between the simulated bulk densities and our refined theory.

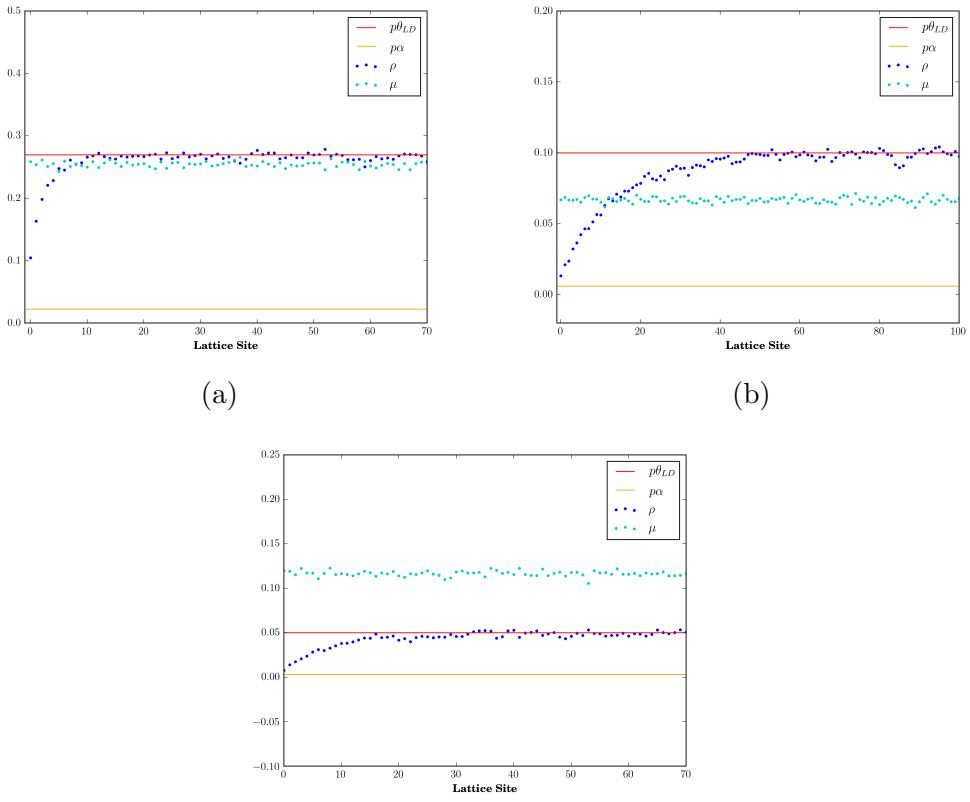

Figure 2.13: (a) Detail of the left tip of the lattice of Figure 2.12(a). The continuous red line indicates the refined mean field predicted value of the ρ density in the bulk, while the orange line is the value that the density would assume in a standard TASEP with entrance rate of $p\alpha$. In the plots (b) and (c) a zoom of the left lattice end is also presented, for $\alpha = 0.01$, $q = 0.06$ and different values of p: $p = 0.6$ in (b) and $p = 0.3$ in (c). In all three cases, we witness a non constant fast partciles density in the region near the left lattice end: it grows from a value of $\rho = p\alpha$ to the predicted one of $\rho = p\alpha/q$ in the bulk, marked, respectively, by the orange and red continous lines.

Chapter 3

Heterogeneous TASEP and LK

Since we are interested in modeling motor dynamics on microtubules, we want our model to be as close as possible as the real process inside cells. In order to achieve this goal, one first step is to introduce, on top of our TASEP-like dynamics, also the possibility of attachment and detachment of motors on and from the lattice, as it happens in the real biological system, where motors can attach to the microtubule from the sourrounding medium and can detach to it, after walking for a fraction of the lane.

3.1 The Langmuir Kinetics

In literature, the attachment-detachment process is reffered to as *Langmuir Kinetics* (LK) and, when considered alone, on a 1D lattice, leads to the system that we're now going to briefly describe.

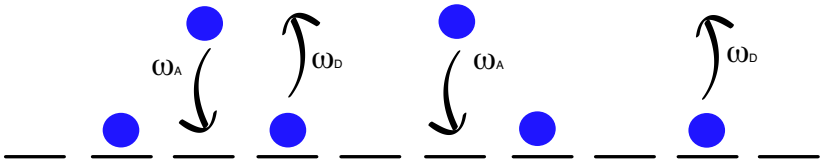

Figure 3.1: Lattice with Langmuir Kinetics

As seen in Fig. 3.1, particles attach at rate ω_A and detach at rate ω_D form any latice site. As before, we are interested in the density profile at the steady state. Defined n_i the occupation variable for the ith site, the time evolution of its avarage is easily derived:

$$\frac{d}{dt}\langle n_i \rangle = \omega_A(1 - \langle n_i \rangle) - \omega_D \langle n_i \rangle \tag{3.1}$$

so that, in the steady state ($\frac{d}{dt}\langle n_i\rangle = 0$), it's easy to compute the avarage density:

$$\langle n_i\rangle_{ss} = \frac{K}{K+1} \tag{3.2}$$

where K is defined as $K := \omega_A/\omega_D$. In the case where we have two species of

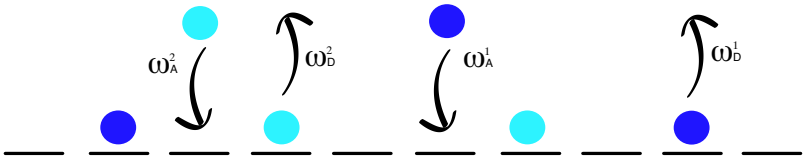

Figure 3.2: Lattice with 2 Species Langmuir Kinetics

particles, with their own attachment and detachment rates, $\omega_A^1, \omega_A^2, \omega_D^1, \omega_D^2$ (see Fig. 3.2), things become only slightly more complex. with the same notation for the two species occupation as before, we have that:

$$\begin{aligned}\frac{d}{dt}\langle n_i\rangle &= \omega_A^1(1-\langle n_i\rangle-\langle m_i\rangle) - \omega_D^1\langle n_i\rangle \\ \frac{d}{dt}\langle m_i\rangle &= \omega_A^2(1-\langle n_i\rangle-\langle m_i\rangle) - \omega_D^2\langle m_i\rangle\end{aligned} \tag{3.3}$$

And equating the time derivatives to 0, we can again easily obtain the steady state density profiles:

$$\begin{aligned}\langle n_i\rangle_{ss} &= \frac{K_1}{1+K} \\ \langle m_i\rangle_{ss} &= \frac{K_2}{1+K}\end{aligned} \tag{3.4}$$

where we have $K_{1/2} := \omega_A^{1/2}/\omega_D^{1/2}$ and $K := K_1 + K_2$. All these are exact results, and simulations agree perfectly with them.

3.2 TASEP and LK

As stated in the introduction of the chapter, we now want to study the steady state densities of a two species TASEP coupled with LK. The model we are interested in, therefore, is the one represented in Figure 3.3: particles can

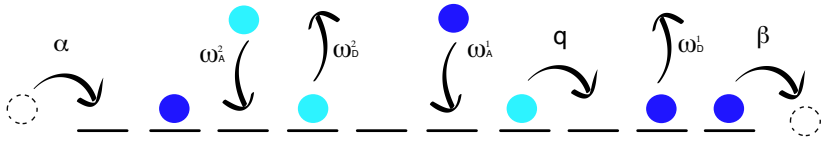

Figure 3.3: Lattice with 2-TASEP dynamics coupled with LK

enter the lattice at the first site with rate α (more precisely, with rate $p\alpha$ for the fast particles and $(1-p)\alpha$ for the slow ones), leave it from the last site with rate β, attach and detach from any other site respectively with rates $\omega_A^1, \omega_A^2, \omega_D^1, \omega_D^2$, and jump forward if the next site is empty, with hopping rate of 1 and $q < 1$, respectively for the particles of the first and second species.

Again, as for the model analyzed in the previous sections, we are now interested in deriving an accurate expression for the two species densities in the steady state.

3.2.1 Mean Field Analysis

As already done before, one can easily derive the time evolution of the density profiles in the bulk:

$$\begin{aligned}
\frac{d}{dt}\rho_i &= \langle n_{i-1}(1-n_i-m_i)\rangle - \langle n_i(1-n_{i+1}-m_{i+1})\rangle + \\
&+ \omega_A^1(1-\langle n_i\rangle - \langle m_i\rangle) - \omega_D^1\langle n_i\rangle \\
\frac{d}{dt}\mu_i &= q\langle m_{i-1}(1-n_i-m_i)\rangle - q\langle m_i(1-n_{i+1}-m_{i+1})\rangle + \\
&+ \omega_A^2(1-\langle n_i\rangle - \langle m_i\rangle) - \omega_D^2\langle m_i\rangle
\end{aligned} \tag{3.5}$$

whereas for the first and last lattice sites, we have the same equations as in (1.7) and (1.6):

$$\begin{aligned}
\frac{d}{dt}\rho_1 &= p\alpha\langle 1-n_1-m_1\rangle - \langle n_1(1-n_2-m_2)\rangle \\
\frac{d}{dt}\mu_1 &= (1-p)\alpha\langle 1-n_1-m_1\rangle - q\langle m_1(1-n_2-m_2)\rangle \\
\\
\frac{d}{dt}\rho_N &= \langle n_{N-1}(1-n_N-m_N)\rangle - \beta\langle n_N\rangle \\
\frac{d}{dt}\mu_N &= q\langle m_{N-1}(1-n_N-m_N)\rangle - \beta\langle m_N\rangle
\end{aligned} \tag{3.6}$$

As expected, we find the that in order to calculate the time evolution of the avarage occupation, we need also the higher moments of its distribution.

Although a mean field approximation has failed in the analysis of the two species TASEP, it may nonetheless be worth trying again with such an approach in this case, if we consider that the Langmuir kinetics may reduce the contributions due to the correlations. With this hope, we try, therefore, once more to perform a mean field analysis.

With the same notation as before, under the mean field assumption and in the steady state ($\frac{d}{dt}\rho_i = \frac{d}{dt}\mu_i = 0$), equations (3.5) become:

$$\begin{aligned} 0 &= \rho_i(1-\rho_i-\mu_i) - \rho_i(1-\rho_{i+1}-\mu_{i+1}) + \\ &+ \ \omega_A^1(1-\rho_i-\mu_i) - \omega_D^1\rho_i \\ 0 &= q\mu_i(1-\rho_i-\mu_i) - q\mu_i(1-\rho_{i+1}-\mu_{i+1}) + \\ &+ \ \omega_A^2(1-\rho_i-\mu_i) - \omega_D^2\mu_i \end{aligned} \tag{3.7}$$

In order to be able to find an explicit expression for the desities ρ_i and μ_i which solve these equations, it is useful to consider the continuum limit of the system: i.e. we coarse grain the lattice, considering infinitely many sites ($N \to \infty$) while keeping the lenght of the lattice, L, constant (for simplicity we will set $L = 1$). For large N, we will then consider the quasi-continuoous variable $x := i/N$ instead of i, and rewrite the equations (3.7) expanding in the lattice constant $\varepsilon := L/N = 1/N$:

$$\begin{aligned} 0 =& \varepsilon\partial_x[\rho(x)(1-\theta(x))] - \omega_A^1(1-\theta(x)) + \omega_D^1\rho(x) + o(\varepsilon^2) \\ 0 =& \varepsilon\partial_x[\mu(x)(1-\theta(x))] - \frac{\omega_A^2}{q}(1-\theta(x)) + \frac{\omega_D^2\mu(x)}{q} + o(\varepsilon^2) \end{aligned} \tag{3.8}$$

An important remark to make before proceeding is that, as explained in detail in [13], in order for the LK process not to become dominant over the TASEP one in the infinite lattice sites limit, we need the attachment and detachment rates to scale as $1/N$: $\omega_{A/D}^{1/2} = \Omega_{A/D}^{1/2}/N$, for some constant $\Omega_{A/D}^{1/2}$. The reason behind this is that if the LK rates remain constant, then the particles on the lattice will, on average, always spend the same amount of time on it, travelling for the same average number of sites, before detaching. But, as the number of sites increases, such average number will become a negligible fraction of the total lattice lenght, so that the TASEP dynamics will be dominated by the LK one, and its effects will no longer be relevant.

Therefore, we rewrite $\omega_{A/D}^{1/2}$ as $\omega_{A/D}^{1/2} = \varepsilon\Omega_{A/D}^{1/2}$, so that the equations (3.8), at first order in ε, become:

$$\begin{aligned} 0 =& \partial_x[\rho(x)(1-\theta(x))] - \Omega_A^1(1-\theta(x)) + \Omega_D^1\rho(x) \\ 0 =& \partial_x[\mu(x)(1-\theta(x))] - \frac{\Omega_A^2}{q}(1-\theta(x)) + \frac{\Omega_D^2}{q}\mu(x) \end{aligned} \tag{3.9}$$

whereas, for what concerns the boundary conditions at the left and right ends of the lattice, equations (1.6) in the continuum limit and at first order in ε translate into:

$$\begin{aligned} & p\alpha(1-\theta(0)) - \rho(0)(1-\theta(0)) = 0 \\ & \frac{(1-p)}{q}\alpha(1-\theta(0)) - \mu(0)(1-\theta(0)) = 0 \end{aligned} \tag{3.10}$$

which gives:

$$\begin{aligned} \rho(0) &= p\alpha \\ \mu(0) &= \frac{1-p}{q}\alpha \\ \theta(0) &= \alpha(p + \frac{1-p}{q}) \end{aligned} \tag{3.11}$$

while equations (1.7) become:

$$\begin{aligned} & \rho(1)(1-\theta(1)) - \beta\rho(1) = 0 \\ & \mu(1)(1-\theta(1)) - \frac{\beta}{q}\mu(1) = 0 \end{aligned} \tag{3.12}$$

As pointed out in [13], at first order in ε, we obtain a system of first order differential equations for the densities $\rho(x)$ and $\mu(x)$, but we have two different boundary conditions: one at $x = 0$ and one at $x = 1$: the problem is overdetermined.

On top of that, in our case, we have also an additional issue concerning the right boundary. If we try to solve (3.12) for $\theta(1)$, in fact, we obtain two different results depending on whether we assume $\rho(1) \neq 0$ and, therefore, obtain $\theta(1)$ from the first equation of the (3.12), or, instead, we assume

$\mu(1) \neq 0$ and get $\theta(1)$ from the second one. In the first case, in fact, we obtain:

$$\begin{aligned} \theta(1) &= 1 - \beta \\ \rho(1) &= 1 - \beta \\ \mu(1) &= 0 \end{aligned} \tag{3.13}$$

while, in the second we get:

$$\begin{aligned} \theta(1) &= 1 - \frac{\beta}{q} \\ \rho(1) &= 0 \\ \mu(1) &= 1 - \frac{\beta}{q} \end{aligned} \tag{3.14}$$

What is interesting to notice is that, according to these results, no matter which boundary condition among the (3.13) and (3.14) is satisfied, in both cases we witness species segregation at the rightmost end of the microtubule, a phenomenon that has been described also by Pinkoviezky and Gov [17].

To obtain the mean field densities at the steady state we should now solve equations (3.8). A possible way to proceed is the one exploited in [17], which seems to give nice results which are in good agreement with the simulations. However, in this work, the authors were considering different species differing only in the LK rates and not in the hopping ones. And, although at some point they claim that their mean field results apply also in the case of different hopping rates, this is not further justified and, therefore, before trying anything else, we would like to test the validity of the mean field approach in our case.

To this end, a sensible approach is to rewrite equations (3.9) in a region of the parameters space where they simplify and where it is possible to easily get an analytic solution.

Such a result is achievable for various choices of the LK parameters. One particular region of the LK rates that we found interesting to explore is the one defined by the following constraints:

$$\begin{aligned} \Omega_D^1 &= \frac{\Omega_D^2}{q} \\ \Omega_D^1 &= \Omega_A^1 + \frac{\Omega_A^2}{q} \end{aligned} \tag{3.15}$$

In this region, in fact, if we define $\Omega := \Omega_D^1$ and sum equations (3.9), we obtain a differential equation for $\theta(x)$ which depends only on Ω:

$$(2\theta(x) - 1)(\partial_x\theta(x) - \Omega) = 0 \tag{3.16}$$

This first order differential equation, with 2 different boundary conditions, is studied in detail in [13], for it is the equation obtained in the mean field and continous limit for a standard TASEP coupled with LK, in the symmetric case: $K := \Omega_A/\Omega_D = 1$. Depending on the values of Ω, α and β, one expects different behaviour of the density profile with different matchings of the three solutions of (3.16). However, it is important to stress that while the contraints (3.15) leave us with 2 free LK parameters – Ω and, let's say, $K_1 := \Omega_A^1/\Omega_D^1$ – the solutions of (3.16) only depend on Ω and the boundary conditions (i.e. on α and β). So that, now, if the mean field approximation provides, indeed, an accurate description, we expect not only to recover the density profiles obtained in [13] as solutions of (3.16), but also that this profiles do not depend on K_1.

3.2.2 Simulations

Based on the considerations made in the last section, we now want to test the mean field prediction. To this end, we set the LK parameters so that the conditions (3.15) are satisfied and simulate the system evolution for different values of K_1 till reaching a state near to stationariety, and then compute the time avarages for the occupations along the lattice. What we expect, as said, is not only to recover the profiles described in [13], but also that all the curves coincide. The results of such simulations are presented in the plot in Figure 3.4.

The first thing that strikes the eye as one looks at these plots is that the profiles obtained for different values of K_1 are not compatible with each other. The only regions where they agree, in fact, are the plateaux in the middle of the lattice and the right tip of the lattice, where they assume a linear behaviour. As one could expect, the behaviour of the density profiles in these regions is exactly the one predicted by the mean field result represented by equation (3.16): for the choosen values of Ω, α and β, in fact, equation (3.16), together with the boundary conditions, yields a density profile which is constant in the bulk – specifically with a value of $\theta(x) = 1/2$ – and that linearly increases in the last section of the lattice, with a slope given by Ω, more precisely: $\theta_\beta(x) = \Omega(x - 1) + 1 - \beta/q$, where we have chosen the right boundary condition to be given by equations (3.14), rather than (3.13), because, for this particular choice of the LK rates, we have segregation at the

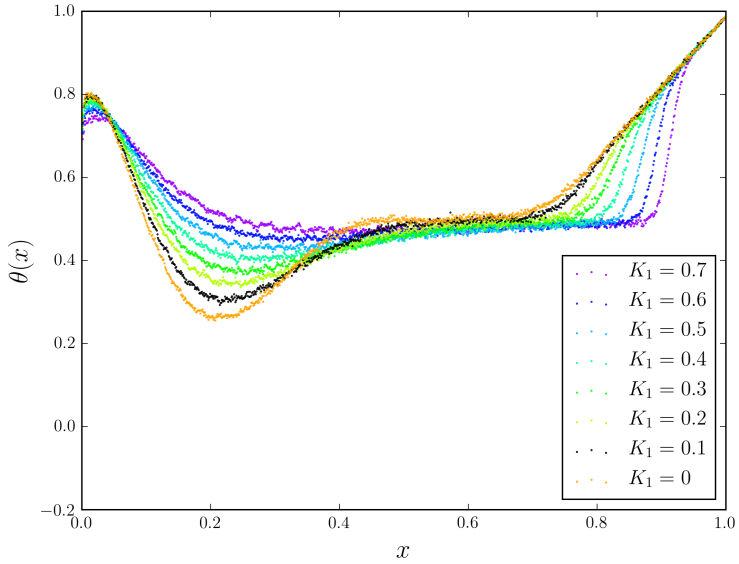

Figure 3.4: Simulated total density profiles for $N = 1000$, $\Omega = 1.7$ and different values of K_1.

rightmost tip with the slow particles taking over the fast ones – see Figure 3.6. As an example, this expected behaviour is plotted against the simulations data for $K_1 = 0$ in Figure 3.5.

What is clear from the plots in Figures 3.4, 3.5 and 3.6 is that, also when LK is added to the model – at least for our choice of the LK rates (3.15) – the diffenrence between the hopping rates of the two species increases sensibly the contribution to the steady state density profiles of the correlations, affecting the accuracy of the mean field predictions.

In particular, for the specific choices of the parameters – which, being the total phase space 8-dimensional, is by no means representative for the general behaviour of the system – we observe two interesting phenomena.

The first one is the minimum in the density in the first part of the lattice, caused by the fast decrease of the first species particles, whose average density decays from the left tip value (determined by the entrance rate α) to the bulk value, which is, on contrary, determined by the LK rates.

The second phenomenon is connected with the species segregation. Looking at the total density plots in Figure 3.4, in fact, we have already observed that, near the end of the lattice, the density profiles seems to agree perfectly with the mean field prediction. And, indeed, it does so, and the reason for

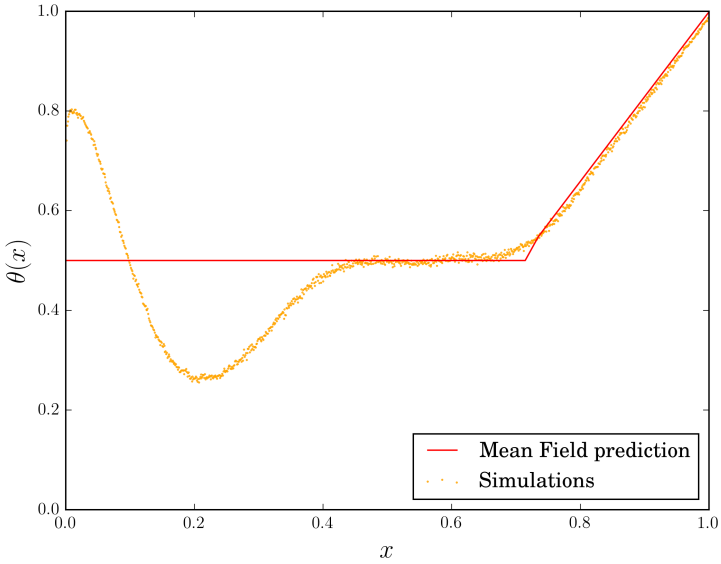

Figure 3.5: In this plot, the density profile of Figure 3.4 for $K_1 = 0$ (dotted data) is plotted against the result predicted by the mean field theory (continous red line).

that is immediately clear if one plots separately the fast and slow particle densities, as it is done for some values of K_1 in Figure 3.6. From these plots, in fact, one can see that the region of the lattice in which the total density $\theta(x)$ start assuming the linearly increasing behaviour predicted by the mean field theory coincides exactly with the region in which the fast particle density starts decreasing until vanishing completely by the end of the lattice. This means that, in this last fraction of the lattice, there are almost no fast particles left, resulting in the fact that, here, only one species of particles is present in the system, so that is no surprise that the mean field approximation works well. As K_1 is increased, in fact, the fast particles populate also further regions of the lattice – as we can clearly see from Figure 3.6(b) and 3.6(c) – and this leads to a deviation from the mean field prediction that propagates further in the lattice and closer to the lattice right end.

This suggests that segregation is, in fact, not so easily justified just by means of equations (3.13) and (3.14). Intuitively, what happens at the end of the lattice is that, given the low β value, and since the fast particles detach more often than the slow ones, the slow hopping particles tend to occupy all free sites, so that the fast particles can hardly reattach, resulting in a decay

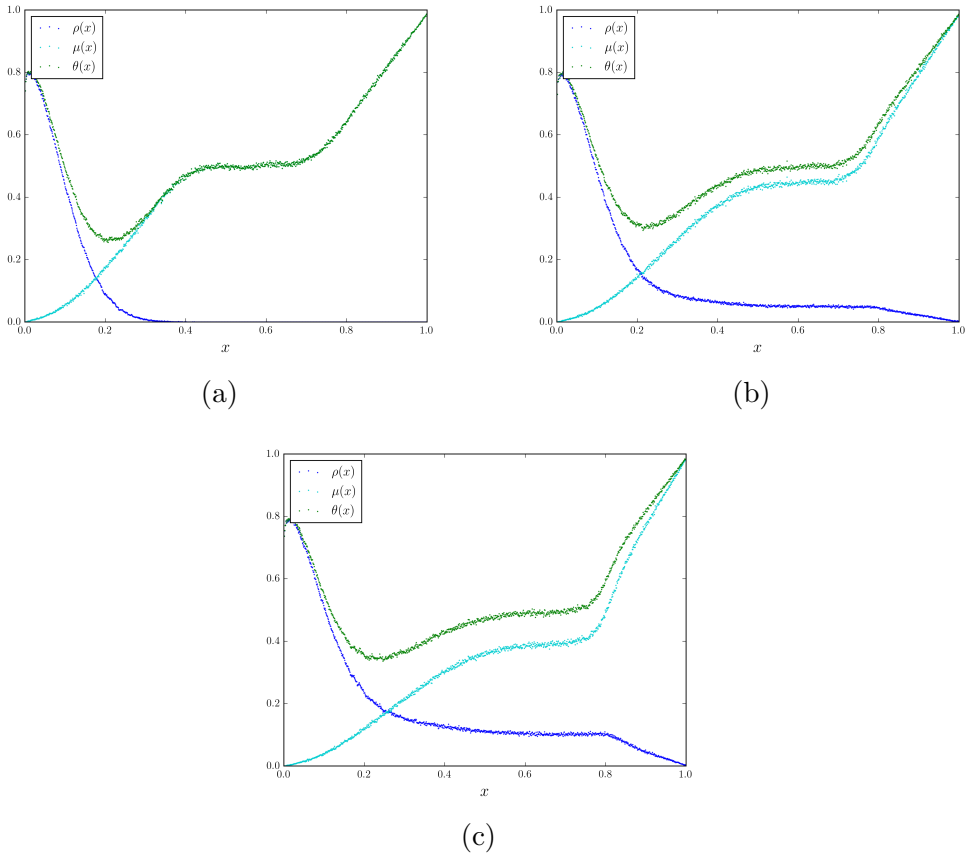

Figure 3.6: Density profiles for the two species $\rho(x)$ and $\mu(x)$ (blue and light blue respectively) together with the total density $\theta(x)$ (green), for three different values of K_1: $K_1 = 0$ (a), $K_1 = 0.1$ (b) and $K_1 = 0.2$ (c). In all cases (as well as for all the other values of K_1 plotted in Figure 3.4), we witness species segregation at the end of the lattice. In particular, the slow particles take over the fast ones, whose density decays before reaching the end of the lattice.

of the ρ-density. If this interpretation is correct, therefore, we can conclude that species segregation is driven by LK and depends strongly on the choice of the dynamic parameters.

At the light of this, another interesting parameter space region to look at is the one where the relative fraction of fast particles in the system is kept equal to the one given by the fraction of the entry rates p. This is achieved by setting:

$$\begin{aligned} \Omega_A^1 &= p\Omega_A \\ \Omega_A^2 &= (1-p)\Omega_A \\ \Omega_D^1 &= \Omega_D^2 = \Omega_D \end{aligned} \tag{3.17}$$

for some Ω_A and Ω_D.

In this regime, we recovered the behaviour that has also been found in the standard TASEP coupled with LK, for example by Frey and colleagues in [16] and [13]. We found, namely, that for particular choices of the parameters, a domain wall appears in the system, separating a low density region from a high density one, as can be seen in the plots of Figure 3.7, from which we see not only that there is no segregation of species at the end of the lattice, but also that the single species densities continue to obey the relations 1.12 throughout the lattice, excluding the left tip, where a similar phenomenon to the one analized previously appears.

These findings confirm what we had imagined before: being the parameter space so vast, the phenomenology of the model is extremely variegated and rich. For this reason – together with the fact that a simple mean field analysis seems not to provide accurate predictions for every choice of the parameters – a detailed and complete analysis of the phase space of this model appears to be better suited for further work and research.

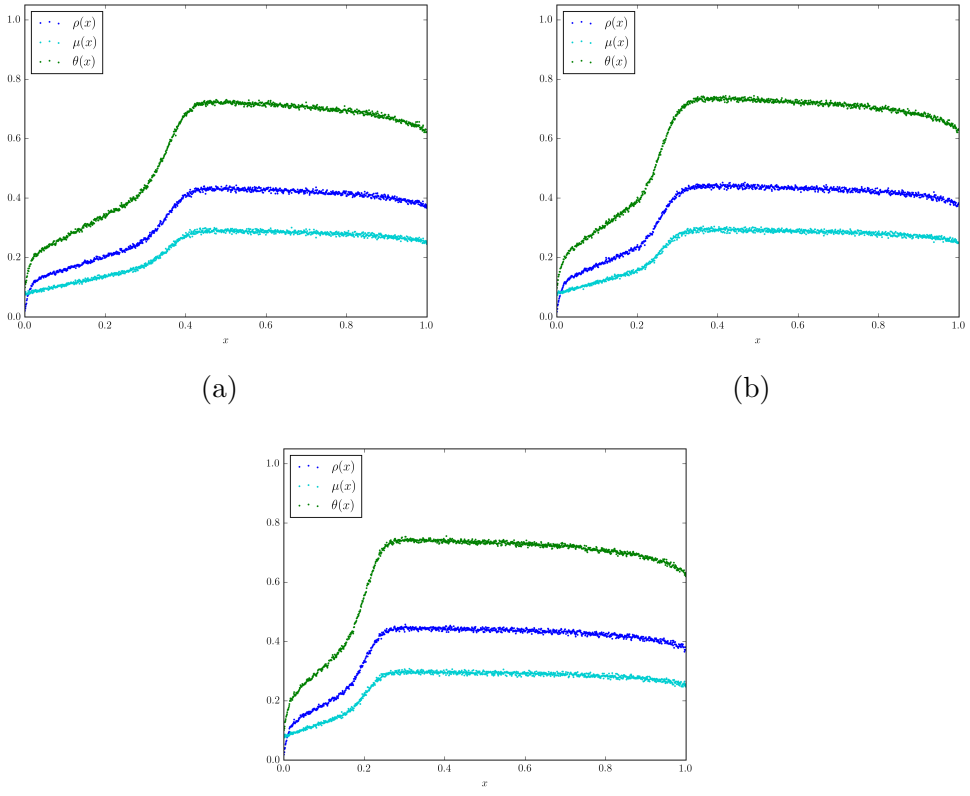

(a) (b)

(c)

Figure 3.7: Density profiles for LK parameters given by 3.17, with $\alpha = 0.016$, $\beta = 0.048$, $q = 0.08$, $p = 0.6$, and different choiches of Ω_A and Ω_D: (a) $\Omega_A = 5.7 \times 10^{-6}$, $\Omega_D = 1.9 \times 10^{-6}$; (b) $\Omega_A = 7.5 \times 10^{-6}$, $\Omega_D = 2.5$; (c) $\Omega_A = 1.11 \times 10^{-5}$, $\Omega_D = 3.7 \times 10^{-6}$. We can see that, in this case, the relations 1.12 are satisfied throughout the lattice, till the right tip, so that no species segregation is present. We notice that, instead, a domain wall appears in the bulk, separating a low density region on the left from an high density one on the right, and giving rise to a profile density which has the exact same shape as the one found by Frey and collaborators in [13].

Conclusions

Motivated by the fact that heterogeneity of motor properties (in particular of their average velocity) is found in biological systems, we decided to analyze a modified version of the standard TASEP, where various species of particles, differing in the hopping rate, are allowed to walk on the same lattice.

In the first part we found that having particles with different hopping rates has a big impact on correlations of the occupation variables, so that a simple mean field analysis fails to predict accurate values of the steady state densities and average current. We discovered that having slow particles in the system leads to jamming and clustering phenomena. We then exploited such a clustering behaviour shown by the system in certain regions of the parameters space to derive a refined mean field theory, which gave very accurate results.

Unfortunately, as it is shown by the plot in Figure 2.5, the predictions of our theory start deviating from the simulation results as the slow hopping rate q approaches 1. While for $q \to 1$ the mean field description can be regarded as a good enough approximation, for intermediate values of the slow hopping rate neither of the two theories provide satisfying results. What one expects, though, is just a quantitative change of the critical values of the entrance and exit parameters. To get a quantitative estimate of such a change, further research could focus on trying to estimate the contributions of correlations in such a regime as well, so that the exact phase space for the heterogenous TASEP would be known for all regimes.

We then went on to analyze what happens when an heterogeneous TASEP is coupled to LK. In particular, we allowed the two species of particles to also have different attachment and detachment rates. In doing so, we obtain an eight-dimensional parameter space, which is, as one can imagine, very vast to explore.

Before trying to solve the general model's equations in the mean field limit, we wanted to test if such an approach was even worth the try. We therefore decided to restrict ourselves to a two dimensional surface of the LK space, where the differential equation in the continous limit for the total

density θ becomes easily solvable. The simulations showed that, in this regime, the system shows very interesting behaviours non predicted by the mean field analysis, one of these being species segregation at the right tip of the lattice.

Further exploration of the parameter space showed that, with different choices of the LK rates, it is possible to maintain the relations 1.12 trhough the lattice. Moreover, in such a regime, we also observed the emergence of a domain wall in the bulk of the lattice, separating a low density region on the left from an high density one on the right. This phenomenology is in all similar to the one observed by Frey and colleagues in the study of the standard TASEP coupled with LK [13].

These findings suggest that the addition of a second species, which can have its own dynamical rates, only greately enriches the possible behaviour and phenomenology shown by the model, making a simple mean field analysis less effective in certain regimes. Future work and research could focus on trying to go beyond a phenomenological analysis of the heterougenous TASEP coupled with LK, in particular in biologically interesting regimes.

Acknowledgments

A master thesis is hardly the result of a single person's efforts, rather are the help and contribution of many people that make it possible. In this section, therefore, I would like to thank all the people that helped me in realizing this thesis and that have been essential and precious support during the last years.

First of all, I would like to thank Professor Erwin Frey for giving me the great opportunity to work in his amazing group. Secondly, many thanks go to Matthias, who has always helped me with patience, giving me feedbacks on my work, invaluable advice and suggestions. What is sure is that without his help there would be no thesis.

Further and deep thanks go to my family, in particular to my parents, who supported me in any possible way during all my studies. They have always believed in me, being the best parents possible, and I hope I managed to make them proud.

Family is also friends, and there are some friends you could not imagine your life without. Thank you Tommy, for always being there, as the extraordinary person that you are! Thanks also to Costanza, Alberto and Giancarlo†, great friends and models! And infinite thanks to you, dear SüSe: you never stopped believing and supporting me!

Finally, my life in Munich during the TMP would not have been in any way comparable to what it has, without some of the amazing people that I met here and that I am now very happy to be able to call friends. Thank you Fabian, Lea, Chrissy, Federica, Andreas, Hannes, Michi and Lukas.

Bibliography

[1] J. Howard and A. a. Hyman, "Dynamics and mechanics of the microtubule plus end.," *Nature*, vol. 422, pp. 753–8, apr 2003.

[2] J. Hayles and P. Nurse, "A journey into space," *Nat Rev Mol Cell Biol*, vol. 2, pp. 647–656, sep 2001.

[3] I. M. Tolić-Nørrelykke, "Force and length regulation in the microtubule cytoskeleton: lessons from fission yeast," *Current Opinion in Cell Biology*, vol. 22, no. 1, pp. 21 – 28, 2010. Cell structure and dynamics.

[4] J. Howard, *Mechanics of Motor Proteins and the Cytoskeleton*. Sinauer Associates, 2001.

[5] T. Chou, K. Mallick, and R. K. P. Zia, "Non-equilibrium statistical mechanics: from a paradigmatic model to biological transport," *Reports on Progress in Physics*, vol. 74, no. 11, p. 116601, 2011.

[6] E. Nogales, S. G. Wolf, and K. H. Downing, "Structure of the [alpha][beta] tubulin dimer by electron crystallography," *Nature*, vol. 391, pp. 199–203, jan 1998.

[7] B. J. N. Reddy, S. Tripathy, J. Xu, M. Mattson, K. Arabi, M. Vershinin, S. Gross, and C. Hyeon, "Time traces of individual kinesin motors suggest functional heterogeneity," pp. 1–11, 2015.

[8] B. Derrida, E. Domany, and D. Mukamel, "An exact solution of a one-dimensional asymmetric exclusion model with open boundaries," *Journal of Statistical Physics*, vol. 69, no. 3, pp. 667–687, 1992.

[9] R. S. Krapivski, L.K. and E. Ben-Naim, *A Kinetic View of Statistical Physics*. Cambridge University Press, 2010.

[10] B. Derrida, "An exactly soluble non-equilibrium system: The asymmetric simple exclusion process," *Physics Reports*, vol. 301, no. 1–3, pp. 65 – 83, 1998.

[11] R. A. Blythe and M. R. Evans, "Nonequilibrium steady states of matrix-product form: a solver's guide," *Journal of Physics A: Mathematical and Theoretical*, vol. 40, no. 46, p. R333, 2007.

[12] M. Ebbinghaus and L. Santen, "Intracellular transport driven by molecular motors : General mechanisms and defects," *Physics Reports*, vol. 593, pp. 1–59, 2015.

[13] A. Parmeggiani, T. Franosch, and E. Frey, "Totally asymmetric simple exclusion process with Langmuir kinetics," *Physical Review E*, vol. 70, pp. 1–20, oct 2004.

[14] D. Gillespie, "Exact stochastic simulation of coupled chemical reactions," *The journal of physical chemistry*, vol. 93555, no. 1, pp. 2340–2361, 1977.

[15] G. Lakatos and T. Chou, "Totally asymmetric exclusion processes with particles of arbitrary size," *J. Phys. A: Math. Gen.*, vol. 36, no. 8, pp. 2027–2041, 2003.

[16] A. Parmeggiani, T. Franosch, and E. Frey, "Phase Coexistence in Driven One-Dimensional Transport," *Physical Review Letters*, vol. 90, pp. 1–4, feb 2003.

[17] I. Pinkoviezky and N. S. Gov, "Exclusion and hierarchy of time scales lead to spatial segregation of molecular motors in cellular protrusions," *Physical Review Letters*, vol. 118, p. 1–5, jan 2017.

[18] B. Derrida, M. R. Evans, V. Hakim, and V. Pasquier, "Exact solution of a 1d asymmetric exclusion model using a matrix formulation," *Journal of Physics A: Mathematical and General*, vol. 26, no. 7, p. 1493, 1993.

[19] G. Schütz and E. Domany, "Phase transitions in an exactly soluble one-dimensional exclusion process," *Journal of Statistical Physics*, vol. 72, no. 1, pp. 277–296, 1993.

[20] R. Fowler, *Statistical Mechanics*. Cambridge University Press, 1936.